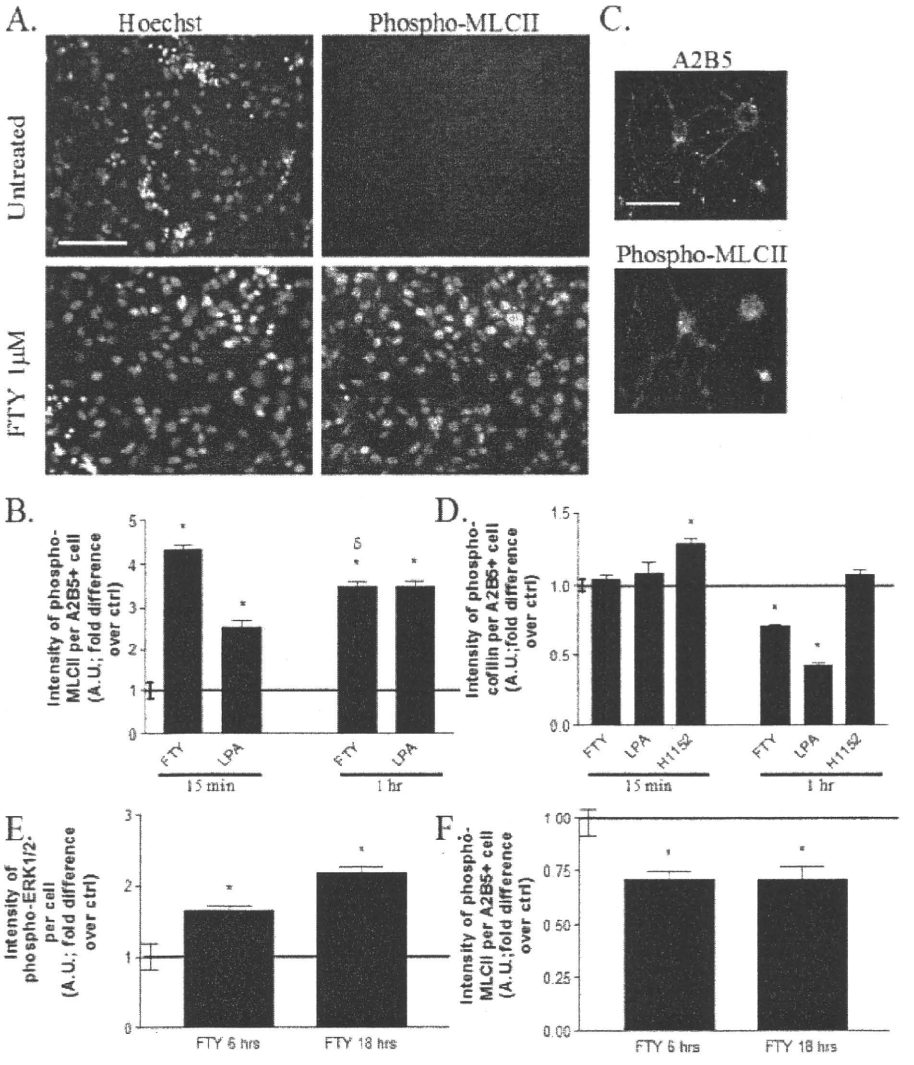


*Fig 3. FTY720-induced changes in process dynamics are associated with activation of proteins associated with Rho GTPase activity. (A) Representative images of untreated (top) and FTY720-treated (1μM, bottom) oligodendrocyte progenitor cells (OPCs) immunostained against the nuclear marker Hoechst (left) demonstrate that 15 minutes of FTY720 treatment increases phospho-myosin light chain (MLC) II staining intensity (right) relative to control. Scale bar = 100μm. (B) Quantification of phospho-MLC II staining intensity per A2B5+ cell at 15 minutes and 1 hour of treatment normalized to untreated control. FTY720 (1μM) and the positive control lysophosphatidic acid (LPA) significantly increased phospho-MLC staining intensity. (C) Double immunostaining demonstrates an increase in phospho-MLC II staining intensity in A2B5-immunopositive OPCs. Scale bar = 50μm. (D) Quantification of phosphocofilin staining intensity per A2B5+ cell normalized to untreated control. FTY720 (1μM) and LPA caused a significant decrease relative to control at 1 hour, whereas the positive control H1152 induced an increase in signal at 15 minutes. *p < 0.05 versus untreated; δp < 0.05 versus 15-minute FTY720-treated. (E) Quantification of phospho-extracellular signal-regulated kinases (ERK) 1 and 2 staining intensity per A2B5+ cell normalized to untreated control. FTY720 (1μM) caused a significant increase relative to control at 6 and 18 hours, with a concomitant decrease in phospho-MLC II (F).*

### *FTY720 Reciprocally Modulates Oligodendrocyte Progenitor Cell Sphingosine-1-Phosphate Receptors 1 and 5 Messenger RNA Levels*

We first used $CD8^+$ T lymphocytes as positive controls for S1P1, S1P4, and S1P5 receptor expression,[30] and Jurkat T cells as a control for S1P3 levels[31] (Fig 6A). In OPCs, we observed that 1μM FTY720 induced a time-dependent regulation of S1P5 versus S1P1 mRNA levels. One day of FTY720 treatment induced a significant downregulation of S1P5 relative to untreated cultures (see Fig 6B) and a concomitant increase in S1P1 mRNA levels (0.23 ± 0.23 and 2.37 ± 0.9-fold over control, respectively) (see Fig 6C). By 4 days of FTY720 treatment, the reverse was observed with an increase in S1P5

and a decrease in S1P1 transcript levels (3.00 ± 0.002 and 0.60 ± 0.002-fold over control, respectively) (see Figs 6B, C). We did observe a decrease in S1P1 and S1P5 transcript levels over time in our untreated cultures (see Figs 6B, C). This may be due to the presence of the cell survival-promoting agent PDGF, shown to induce the production of S1P,[41] which can, in turn, bind S1P receptors and induce their downregulation.

FTY720 caused an upregulation in S1P3 mRNA levels both at 1 and 4 days of treatment (89.5 ± 13 and 1.56 ± 0.06-fold over control, respectively) (see Fig 6D), although levels still remained low relative to S1P1 and S1P5. S1P4 mRNA levels remained undetectable in control and FTY720-treated conditions at 1, 2, and 4 days in culture.

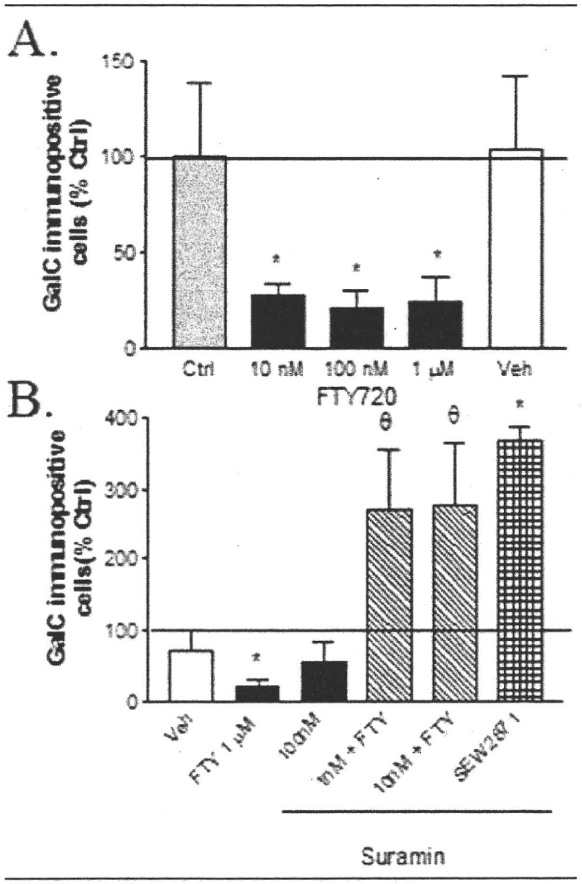


*Fig 4. FTY720 inhibits oligodendrocyte progenitor cell (OPC) differentiation. (A) Quantification of the proportion of galactocerebroside (GalC) immunopositive cells normalized to untreated control (ctrl). Two days of FTY720 treatment (10nM to 1μM) significantly inhibited the maturation of OPCs, not observed with vehicle (veh) treatment. (B) The sphingosine-1-phosphate receptor 3 (S1P3)/S1P5 antagonist suramin (1, 10nM) reversed FTY720-mediated inhibition of OPC differentiation and promoted maturation. SEW2871 (100nM) enhanced differentiation in a comparable manner. *p < 0.05 versus untreated; θp < 0.05 versus FTY720.*

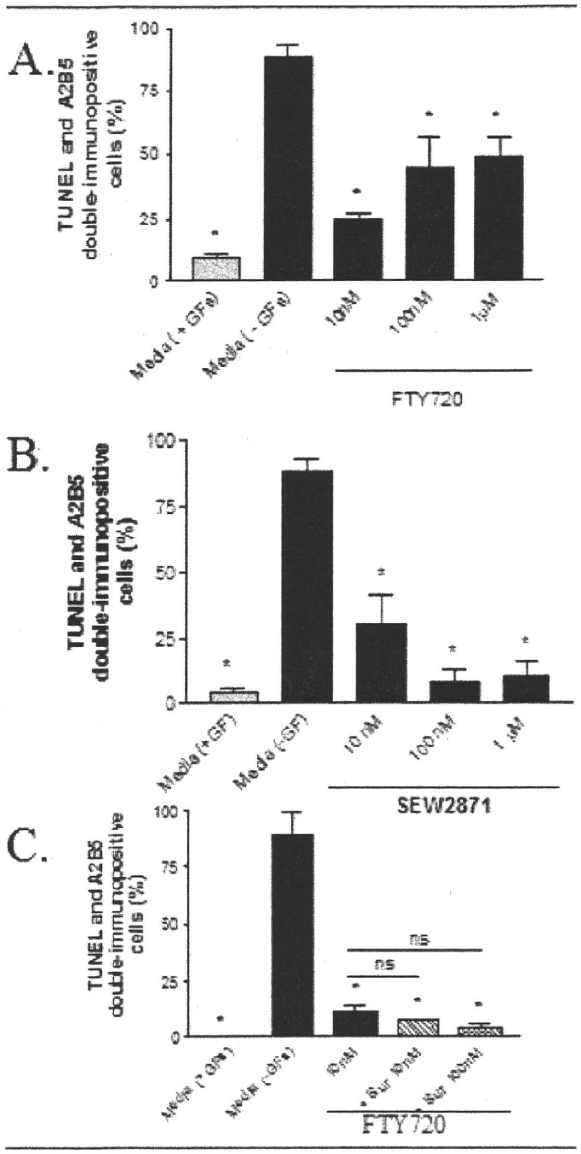


*Fig 5. FTY720 rescues oligodendrocyte progenitor cells (OPCs) from growth factor withdrawal–induced cell death. Growth factor (GF) withdrawal from culture media for 2 days induced an increase in apoptotic terminal deoxynucleotidyltransferase–mediated dUTP nick end labeling (TUNEL)–positive A2B5 OPCs from 10% (+GF) to 89% (−GF). FTY720 treatment (10nM to 1μM) significantly reduced the proportion of apoptotic OPCs. (B) Treatment with the sphingosine-1-phosphate (S1P1)–specific agonist SEW2871 (10nM to 1μM) for 2 days could mimic the FTY720 survival-promoting effect. (C) Cotreatment with FTY720 (10nM) and the S1P3/S1P5 antagonist suramin (10–100nM) could not reverse the FTY720 survival effect. *p < 0.05 versus growth factor withdrawal condition. ns = not significant.*

## Discussion

Our in vitro studies show that FTY720 can exert dose- and time-dependent effects on OPC process extension,

differentiation, and survival, which are all presumed important cellular events in remyelination. The observed functional effects were linked to the modulation of specific S1P receptors.

*FTY720-Induced Modulation of Oligodendrocyte Progenitor Cell Process Extension*

FTY720 induced an initial and gradual process retraction in OPCs that was significantly reversed by cotreatment with an inhibitor of Rho kinase (H1152), the downstream effector of RhoA GTPase, or by uncoupling S1P3 and S1P5 from their G protein with suramin. These findings are consistent with previous studies demonstrating that treating rat O4+ preoligodendrocytes with the endogenous ligand S1P could induce process retraction in an S1P5- and Rho kinase–dependent manner.[23] The FTY720-induced retraction was associated with an expected increase in phosphorylation of the cytoskeletal modulator myosin light chain II, and a simultaneous decrease in phosphorylation of the actin depolymerization factor cofilin. Our findings imply that FTY720 induced process retraction in OPCs through S1P3- and S1P5-mediated activation of RhoA GTPase and Rho kinase, and subsequent activation of cytoskeletal modulators. RhoA activation in rodent oligodendrocytes inhibits remyelination,[42] and Rac1 ablation results in abnormal myelination.[43]

Continued treatment with micromolar concentrations of FTY720 induced process extension in OPCs. Our results are consistent with the transient retraction in S1P-treated rat pre-oligodendrocytes.[23] The FTY720-induced process extension was associated with an increase in phosphorylation of ERK1/2, previously shown to be activated downstream of S1P receptors in oligodendrocytes,[44] and associated with Rac1-dependent process extension.[38–40] The ability

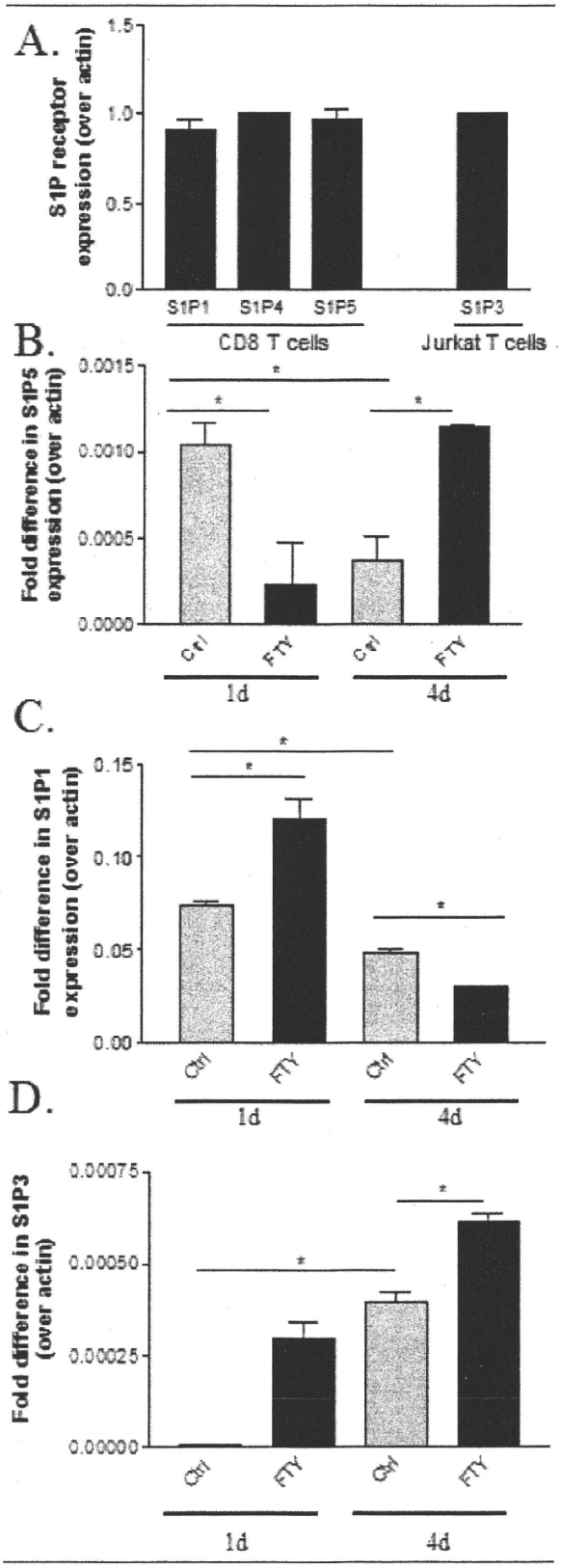


*Fig 6. FTY720 induces time-dependent cycling of sphingosine-1-phosphate (S1P) receptors on human fetal oligodendrocyte progenitor cells (OPCs). Quantitative polymerase chain reaction (qPCR) was performed to determine relative mRNA levels of S1P1, S1P3, and S1P5. All results were normalized to actin levels in the respective sample. CD8 T lymphocytes from two healthy donors were used as positive controls for S1P1, S1P4, and S1P5 mRNA levels; Jurkat T cells served as a control for S1P3 mRNA levels (A). Levels of S1P5 (B), S1P1 (C), and S1P3 (D) were measured from untreated* (gray bars) *and FTY720-treated (1μM,* black bars*) progenitors at 1 and 4 days of treatment. At 1 day of treatment, S1P5 levels decrease relative to control whereas S1P1 increases. At 4 days, the reverse is observed. The decrease in S1P receptor expression over time in untreated cultures is likely due to the presence of platelet-derived growth factor in the media, required for progenitor survival. S1P3 levels continually increased in untreated and FTY720-treated cultures (D). *$p < 0.05$. S1P4 levels remained undetectable in all conditions at all time points.*

of the S1P1-specific agonist SEW2871 to mimic the extension signifies that S1P1-mediated signaling is sufficient to induce this phenomenon in OPCs. S1P1-associated signaling has also been linked with neuronal process extension.[24] Our findings implicate S1P1 and Rac1 GTPase in the FTY720-induced extension.

*FTY720-Mediated Inhibition of Oligodendrocyte Progenitor Cell Differentiation*

FTY720 inhibited OPC differentiation into a more mature oligodendroglial phenotype. This inhibition was alleviated by cotreatment with suramin, suggesting that FTY720 blocked OPC differentiation via S1P5 (±S1P3)-associated signaling. S1P5 signaling in PC12 cells prevents differentiation.[24] Previous studies have demonstrated that S1P5 signaling in Chinese hamster ovary cells decreases basal cyclic adenosine monophosphate levels[45]; increased levels of cyclic adenosine monophosphate have been deemed important for oligodendrocyte differentiation.[46] Conversely, S1P1-mediated signaling was able to enhance the differentiation of our cells. We also observed that FTY720 did not cause OPCs to revert to a less mature phenotype.

*FTY720-Mediated Rescue of Oligodendrocyte Progenitor Cell Death*

We induced OPC cell death by withdrawing all growth factors from the culture media. Others have shown that removing survival factors in culture can induce apoptotic signaling pathways comparable with those stimulated by exogenous insults such as Fas-ligation and ceramide exposure.[47,48] We found that FTY720 could significantly attenuate OPC apoptosis. This was mimicked with SEW2871, but not antagonized with suramin, suggesting that FTY720 could rescue OPCs from cell death in stressful environments via S1P1 signaling. The trophic effect of FTY720 was strongest at lower concentrations; at greater doses, additional receptors and pathways may be activated to counteract the prosurvival responses. We also observed an increase in phosphorylation of the prosurvival kinases ERK1/2 with continued FTY720 treatment, previously associated with Ras GTPase activation and cell survival signaling.[49] Previous studies showed that S1P could not rescue rodent preoligodendrocytes from growth factor withdrawal–induced death.[24] This disparity with our human OPC findings suggests differences in relative S1P receptor levels or associated signaling cascades. Differing sensitivities to S1P receptor modulators have been observed in comparing cell lines transfected with rodent or human S1P receptors.[34] Differences between the two culture systems must also be considered, including differing sample ages, oligodendroglial maturity, isolation and culture techniques, and dependence on growth factors for survival. FTY720 did not affect OPC proliferation, eliminating the possibility that the observed decrease in apoptosis was due to a resistance to growth factor withdrawal–induced death via an increase in mitotic activity.

*FTY720 Modulation of Relative Sphingosine-1-Phosphate Receptor Levels*

We demonstrated that OPCs have relative S1P receptor mRNA levels of S1P1>S1P5>S1P3 and undetectable levels of S1P4. Our results are consistent with S1P1 and S1P5 being most highly expressed on rodent oligodendroglia[21,22]; however, rat OPC S1P5 levels are relatively more abundant than we observed in human OPCs.[50] The relative expression of S1P receptors determines which is preferentially activated and, consequently, the response to FTY720. By quantitative real-time PCR, we observed that S1P5 and S1P1 mRNA levels in OPCs are reciprocally modulated by FTY720 treatment. Short-term FTY720 treatment induced a downregulation of S1P5 and concomitant upregulation of S1P1, whereas the opposite was found with long-term treatment. This may suggest that FTY720 initially preferentially binds to S1P5, inducing its downregulation, and that S1P1 is upregulated as a compensatory mechanism. This upregulation could allow FTY720 to then bind and downregulate S1P1 while upregulating S1P5. Other studies have demonstrated that S1P1-associated signaling can be overridden by other activated S1P receptors, suggesting that S1P1 can only induce functional responses if the remaining S1P receptors are downregulated.[24] The absence of S1P3 downregulation with FTY720 treatment implies that either this receptor is not engaged by the ligand or regulation of S1P3 may differ than for the other receptor isoforms. The absence of S1P4 transcript levels both in untreated and FTY720-treated cultures suggests that this receptor is not implicated in the observed responses to the drug.

Our real-time PCR analysis of S1P receptors and assessment of receptor-specific associated signaling together support changes in S1P receptor protein expression. Our results of receptor modulation are consistent with our functional data implicating an initial S1P5-mediated response (retraction) followed sequentially by S1P1-mediated responses (process extension and survival). Our findings show that, unlike in lymphocytes, chronic FTY720 treatment can induce continuous signaling in OPCs via reciprocal cycling of S1P receptors with presumably opposing signaling pathways.

*Conclusion*

Our studies demonstrate the potential for FTY720 to induce time-dependent modulation of S1P receptors on human OPCs with consequent functional responses that are directly relevant for the remyelination process. These findings support the need to define the potential

impact of chronic FTY720 therapy on remyelination in MS and to consider how S1P signaling may be used as a potential approach to promote remyelination.

This work was supported by the Foundation of the Multiple Sclerosis Society of Canada (J.P.A., T.E.K.), Fondation de Reserche en Sante du Quebec (T.E.K.), the Natural Sciences and Engineering Research Council of Canada, and the Canadian Institutes of Health Research (studentships to V.E.M.), National Institute of Neurological Disorders and Stroke (R21 NS049014, B.S.) and National MS Society (B.S.).

We thank the institutional review board–approved Human Fetal Tissue Repository at the Albert Einstein College of Medicine, Bronx, NY, for providing human fetal tissue. The active phosphorylated form of FTY720 was generously provided by Novartis (Basel, Switzerland).

## References

1. Bruck W, Kuhlmann T, Stadelmann C. Remyelination in multiple sclerosis. J Neurol Sci 2003;206:181–185.
2. Chen JT, Collins DL, Freedman MS, et al. Local magnetization transfer ratio signal inhomogeneity is related to subsequent change in MTR in lesions and normal-appearing white-matter of multiple sclerosis patients. Neuroimage 2005;25:1272–1278.
3. Franklin RJ. Why does remyelination fail in multiple sclerosis? Nat Rev Neurosci 2002;3:705–714.
4. Gensert JM, Goldman JE. Endogenous progenitors remyelinate demyelinated axons in the adult CNS. Neuron 1997;19: 197–203.
5. Roy NS, Benraiss A, Wang S, et al. Promoter-targeted selection and isolation of neural progenitor cells from the adult human ventricular zone. J Neurosci Res 2000;59:321–331.
6. Maeda Y, Solanky M, Menonna J, et al. Platelet-derived growth factor-alpha receptor-positive oligodendroglia are frequent in multiple sclerosis lesions. Ann Neurol 2001;49:776–785.
7. Windrem MS, Roy NS, Wang J, et al. Progenitor cells derived from the adult human subcortical white matter disperse and differentiate as oligodendrocytes within demyelinated lesions of the rat brain. J Neurosci Res 2002;69:966–975.
8. Nunes MC, Roy NS, Keyoung HM, et al. Identification and isolation of multipotential neural progenitor cells from the subcortical white matter of the adult human brain. Nat Med 2003; 9:439–447.
9. Miron VE, Rajasekharan S, Jarjour AA, et al. Simvastatin regulates oligodendroglial process dynamics and survival. Glia 2007;55:130–143.
10. Sanchez T, Hla T. Structural and functional characteristics of S1P receptors. J Cell Biochem 2004;92:913–922.
11. Kappos L, Antel J, Comi G, et al. Oral fingolimod (FTY720) for relapsing multiple sclerosis. N Engl J Med 2006;355: 1124–1140.
12. Davis MD, Clemens JJ, Macdonald TL, et al. Sphingosine 1-phosphate analogs as receptor antagonists. J Biol Chem 2005; 280:9833–9841.
13. Mandala S, Hajdu R, Bergstrom J, et al. Alteration of lymphocyte trafficking by sphingosine-1-phosphate receptor agonists. Science 2002;296:346–349.
14. Beer MS, Stanton JA, Salim K, et al. EDG receptors as a therapeutic target in the nervous system. Ann N Y Acad Sci 2000; 905:118–131.
15. Goetzl EJ, Rosen H. Regulation of immunity by lysosphingolipids and their G protein-coupled receptors. J Clin Invest 2004;114:1531–1537.
16. Liu CH, Thangada S, Lee MJ, et al. Ligand-induced trafficking of the sphingosine-1-phosphate receptor EDG-1. Mol Biol Cell 1999;10:1179–1190.
17. Sawicka E, Dubois G, Jarai G, et al. The sphingosine 1-phosphate receptor agonist FTY720 differentially affects the sequestration of $CD4^+/CD25^+$ T-regulatory cells and enhances their functional activity. J Immunol 2005;175:7973–7980.
18. Webb M, Tham CS, Lin FF, et al. Sphingosine 1-phosphate receptor agonists attenuate relapsing-remitting experimental autoimmune encephalitis in SJL mice. J Neuroimmunol 2004; 153:108–121.
19. Kataoka H, Ohtsuki M, Shimano K, et al. Immunosuppressive activity of FTY720, sphingosine 1-phosphate receptor agonist: II. Effect of FTY720 and FTY720-phosphate on host-versus-graft and graft-versus-host reaction in mice. Transplant Proc 2005;37:107–109.
20. Brinkmann V, Cyster JG, Hla T. FTY720: sphingosine 1-phosphate receptor-1 in the control of lymphocyte egress and endothelial barrier function. Am J Transplant 2004;4: 1019–1025.
21. Yu N, Lariosa-Willingham KD, Lin FF, et al. Characterization of lysophosphatidic acid and sphingosine-1-phosphate-mediated signal transduction in rat cortical oligodendrocytes. Glia 2004; 45:17–27.
22. Terai K, Soga T, Takahashi M, et al. Edg-8 receptors are preferentially expressed in oligodendrocyte lineage cells of the rat CNS. Neuroscience 2003;116:1053–1062.
23. Jaillard C, Harrison S, Stankoff B, et al. Edg8/S1P5: an oligodendroglial receptor with dual function on process retraction and cell survival. J Neurosci 2005;25:1459–1469.
24. Toman RE, Payne SG, Watterson KR, et al. Differential transactivation of sphingosine-1-phosphate receptors modulates NGF-induced neurite extension. J Cell Biol 2004;166: 381–392.
25. Gardell SE, Dubin AE, Chun J. Emerging medicinal roles for lysophospholipid signaling. Trends Mol Med 2006;12:65–75.
26. Lan YY, De Creus A, Colvin BL, et al. The sphingosine-1-phosphate receptor agonist FTY720 modulates dendritic cell trafficking in vivo. Am J Transplant 2005;5:2649–2659.
27. Graler MH, Goetzl EJ. The immunosuppressant FTY720 down-regulates sphingosine 1-phosphate G-protein-coupled receptors. FASEB J 2004;18:551–553.
28. Park SI, Felipe CR, Machado PG, et al. Pharmacokinetic/pharmacodynamic relationships of FTY720 in kidney transplant recipients. Braz J Med Biol Res 2005;38:683–694.
29. Dawson J, Hotchin N, Lax S, et al. Lysophosphatidic acid induces process retraction in CG-4 line oligodendrocytes and oligodendrocyte precursor cells but not in differentiated oligodendrocytes. J Neurochem 2003;87:947–957.
30. Graeler M, Shankar G, Goetzl EJ. Cutting edge: suppression of T cell chemotaxis by sphingosine 1-phosphate. J Immunol 2002;169:4084–4087.
31. Jin Y, Knudsen E, Wang L, et al. Sphingosine-1-phosphate is a novel inhibitor of T-cell proliferation. Blood 2003;101: 4909–4915.
32. Jack CS, Arbour N, Manusow J, et al. TLR signaling tailors innate immune responses in human microglia and astrocytes. J Immunol 2005;175:4320–4330.
33. Ancellin N, Hla T. Differential pharmacological properties and signal transduction of the sphingosine 1-phosphate receptors EDG-1, EDG-3, and EDG-5. J Biol Chem 1999;274: 18997–19002.

34. Niedernberg A, Scherer CR, Busch AE, et al. Comparative analysis of human and rat S1P(5) (edg8): differential expression profiles and sensitivities to antagonists. Biochem Pharmacol 2002;64:1243–1250.
35. Alabed YZ, Grados-Munro E, Ferraro GB, et al. Neuronal responses to myelin are mediated by rho kinase. J Neurochem 2006;96:1616–1625.
36. Pandey D, Goyal P, Siess W. Lysophosphatidic acid stimulation of platelets rapidly induces Ca(2+)-dependent dephosphorylation of cofilin that is independent of dense granule secretion and aggregation. Blood Cells Mol Dis 2007;38:269–279.
37. Lee CW, Rivera R, Dubin AE, et al. LPA(4)/GPR23 is a lysophosphatidic acid (LPA) receptor utilizing G(s)-, G(q)/G(i)-mediated calcium signaling and G(12/13)-mediated Rho activation. J Biol Chem 2007;282:4310–4317.
38. Vouret-Craviari V, Bourcier C, Boulter E, et al. Distinct signals via Rho GTPases and Src drive shape changes by thrombin and sphingosine-1-phosphate in endothelial cells. J Cell Sci 2002; 115:2475–2484.
39. Heffron DS, Mandell JW. Opposing roles of ERK and p38 MAP kinases in FGF2-induced astroglial process extension. Mol Cell Neurosci 2005;28:779–790.
40. Shin EY, Shin KS, Lee CS, et al. Phosphorylation of p85 beta PIX, a Rac/Cdc42-specific guanine nucleotide exchange factor, via the Ras/ERK/PAK2 pathway is required for basic fibroblast growth factor-induced neurite outgrowth. J Biol Chem 2002; 277:44417–44430.
41. Veracini L, Franco M, Boureux A, et al. Two functionally distinct pools of Src kinases for PDGF receptor signalling. Biochem Soc Trans 2005;33:1313–1315.
42. Mi S, Miller RH, Lee X, et al. LINGO-1 negatively regulates myelination by oligodendrocytes. Nat Neurosci 2005;8: 745–751.
43. Thurnherr T, Benninger Y, Wu X, et al. Cdc42 and Rac1 signaling are both required for and act synergistically in the correct formation of myelin sheaths in the CNS. J Neurosci 2006; 26:10110–10119.
44. Hida H, Nagano S, Takeda M, et al. Regulation of mitogen-activated protein kinases by sphingolipid products in oligodendrocytes. J Neurosci 1999;19:7458–7467.
45. Niedernberg A, Blaukat A, Schoneberg T, et al. Regulated and constitutive activation of specific signalling pathways by the human S1P5 receptor. Br J Pharmacol 2003;138:481–493.
46. Palacios N, Sanchez-Franco F, Fernandez M, et al. Intracellular events mediating insulin-like growth factor I-induced oligodendrocyte development: modulation by cyclic AMP. J Neurochem 2005;95:1091–1107.
47. Le Niculescu H, Bonfoco E, Kasuya Y, et al. Withdrawal of survival factors results in activation of the JNK pathway in neuronal cells leading to Fas ligand induction and cell death. Mol Cell Biol 1999;19:751–763.
48. Caricchio R, D'Adamio L, Cohen PL. Fas, ceramide and serum withdrawal induce apoptosis via a common pathway in a type II Jurkat cell line. Cell Death Differ 2002;9:574–580.
49. Banno Y, Takuwa Y, Yamada M, et al. Involvement of phospholipase D in insulin-like growth factor-I-induced activation of extracellular signal-regulated kinase, but not phosphoinositide 3-kinase or Akt, in Chinese hamster ovary cells. Biochem J 2003;369:363–368.
50. Novgorodov AS, El-Alwani M, Bielawski J, et al. Activation of sphingosine-1-phosphate receptor S1P5 inhibits oligodendrocyte progenitor migration. FASEB J 2007;21:1503–1514.
51. Ruffini F, Arbour N, Blain M, et al. Distinctive properties of human adult brain-derived myelin progenitor cells. Am J Pathol 2004;165:2167–2175.

Journal of Neuroscience Research 86:2353–2362 (2008)

# Increase in Dopaminergic Neurons From Mouse Embryonic Stem Cell-Derived Neural Progenitor/Stem Cells Is Mediated by Hypoxia Inducible Factor-1α

**Tae-Sun Kim, Sachiyo Misumi, Cha-Gyun Jung, Tadashi Masuda, Yoshiaki Isobe, Fujiya Furuyama, Hitoo Nishino, and Hideki Hida***

Department of Neurophysiology and Brain Science, Nagoya City University Graduate School of Medical Sciences, Nagoya, Japan

A reliable method to induce neural progenitor/stem cells (NPCs) into dopaminergic (DAergic) neurons has not yet been established. As well, the mechanism involved remains to be elucidated. To induce DAergic differentiation from NPCs, a cytokine mixture (C-Mix) of interleukin (IL)-1β, IL-11, leukemia-inhibitory factor (LIF), and glial-derived neurotrophic factor or low oxygen (3.5% $O_2$: L-Oxy) was used to treat embryonic stem (ES) cell-derived NPCs. Treatment with C-Mix increased the number of tyrosine hydroxylase (TH)-positive cells compared with controls (2.20-fold of control). The C-Mix effect was induced by mainly LIF or IL-1β treatment. Although L-Oxy caused an increase in TH-positive cells (1.34-fold), the combination of L-Oxy with C-Mix did not show an additive effect. Increases in DA in the medium were shown in the presence of C-Mix, LIF, and L-Oxy by high-performance liquid chromatography. Gene expression patterns of neural markers [tryptophan hydroxylase (TPH), GAD67, GluT1, β-tubulin III, glial fibrillary acidc protein, and TH] were different in C-Mix and L-Oxy treatments. Because increases in hypoxia-inducible factor (HIF)-1α protein were found in both treatments, we investigated the effect of HIF-1α on differentiation of NPCs to DAergic neurons. Inhibition of HIF-1α by the application of antisense oligodeoxynucleotides (ODNs) to NPCs caused a decrease in TH-positive cells induced by LIF treatment. Gene expressions of TH, GAD67, and GluT1 were decreased, and those of TPH, β-tubulin III, and S-100β were increased by treatment with just ODNs, indicating the importance of the endogenous effect of HIF-1α on neuronal differentiation. These data suggest that enhanced differentiation into DAergic neurons from ES cell-derived NPCs was induced by C-Mix or L-Oxy mediated by HIF-1α. 

**Key words:** low oxygen; tyrosine hydroxylase; LIF; antisense-oligodeoxynucleotides

Parkinson's disease (PD), a common neurodegenerative disease, is caused by the selective loss of dopaminergic (DAergic) neurons in the substantia nigra pars compacta and the subsequent striatal deficiency of DA. Current treatments for PD include various drug therapies such as L-dopa and DA agonists, during the early stages of the disease, and deep brain stimulation and neural transplantation in the later stages of the disease (Dunnett and Bjorklund, 1999; Carvey et al., 2001; Arenas, 2002; Lindvall, 2003). Neural progenitor/stem cells (NPCs) prepared from fetal brain as neurospheres are promising candidates for use as donor cells in transplantation therapy for PD (Svendsen et al., 1997; Sanchez-Pernaute et al., 2001; Storch et al., 2001; Arenas, 2002; Lindvall, 2003). Although NPCs have the capacity to differentiate into DAergic neurons, there are several practical limitations. For example, most transplanted NPCs do not survive well in the host brain (Castilho et al., 2000), and most cells that do survive differentiate into glial cells and only very rarely into neurons (Nishino et al., 2000; Yang et al., 2002). A reliable method of inducing NPCs into DAergic neurons has yet to be established.

Recent studies have reported that DAergic neurons can be generated from fetal midbrain NPCs in the presence of neurotrophic factors, cytokines, and low oxygen in vitro (Beck et al., 1995; Ling et al., 1998; Studer et al., 1998, 2000; Storch et al., 2001; Carvey et al., 2001; Farkas et al., 2003). Cytokine mixtures of interleukin (IL)-1, IL-11, leukemia inhibitory factor (LIF),

Contract grant sponsor: Ministry of Education, Culture, Sports, Science and Technology (MECSST) of the Japanese Government; Contract grant number: 13073-2125-14 (to H.N., H.H.); Contract grant number: 15200026 (to H.N.); Contract grant sponsor: Japan Society for the Promotion of Science (JSPS); Contract grant number: 14780581 (to H.H.); Contract grant number: 16500203 (to H.H.).

*Correspondence to: Hideki Hida, MD, PhD, Department of Neurophysiology and Brain Science, Nagoya City University Graduate School of Medical Science, Nagoya 467-8601, Japan.
E-mail: hhida@med.nagoya-cu.ac.jp

Received 28 September 2007; Revised 28 December 2007; Accepted 20 January 2008

**Published online 25 April 2008 in Wiley InterScience (www.interscience.wiley.com). DOI: 10.1002/jnr.21687**

and glial-derived neurotrophic factor (GDNF) have been shown to enhance the number of tyrosine hydroxylase (TH)-positive cells in mesencephalic NPCs (Ling et al., 1998; Potter et al., 1999; Carvey et al., 2001; Storch et al., 2001). Low physiological oxygen in fetal brain enhances neurogenesis and differentiation of NPCs into DAergic neurons (Studer et al., 2000). However, the molecular mechanism of DAergic differentiation induced by cytokine mixtures and low oxygen remains unknown (Milosevic et al., 2005).

DAergic neurons are induced from mouse embryonic stem (ES) cells in vitro by retinoic acid (RA) treatment (Bain et al., 1995; Li et al., 1998), by the stromal cell-derived inducing activity (SDIA) method (Kawasaki et al., 2000), and by the five-step method (Lee et al., 2000). It has been reported that cells derived from ES cells maintain their potential to differentiate into DAergic neurons after expansion in vitro (Chung et al., 2006). Insofar as a relatively high proportion of NPCs can be obtained by sequential differentiation in the five-step method, this technique appears to be suitable for investigating the mechanism of DAergic neuron differentiation from NPCs.

In this study, we first investigated whether cytokine mixtures (C-Mix: IL-1β, IL-11, LIF, GDNF) or low oxygen (L-Oxy), similar to the level found in fetal brain (3.5%), induced differentiation of ES cell-derived NPCs to DAergic neurons. We then investigated the differentiation mechanism.

## MATERIALS AND METHODS

### Cell Culture of ES Cell-Derived NPCs

Differentiation of mouse ES cells into DAergic neurons was carried out using the five-step method as reported by the McKay group (Lee et al., 2000) with some modifications (Jung et al., 2004). Briefly, mouse ES cells (D3 cell line, $5 \times 10^5$ cells/ml) were grown on gelatin-coated dishes with 1,000 U/ml ESGRO (Chemicon, Temecula, CA) in ES cell medium: serum-free Dulbecco's modified Eagles's medium (DMEM; Sigma, St. Louis, MO) supplemented with 15% fetal calf serum (FCS), 2 mM L-glutamine (Invitrogen, Carlsbad, CA), 1× nonessential amino acid (Invitrogen), 0.1 mM 2-mecaptoethanol, 50 U/ml streptomycin, and 50 μg/ml penicillin (stage 1). To induce embryoid bodies (EBs), ES cells were dissociated by 0.05% trypsin and 1 mM EDTA in phosphate-buffered saline (PBS), plated onto nonadherent Petri dishes at a density of $1 \times 10^4$ cells/cm$^2$, and cultured for 4 days (stage 2). EBs were then transferred to adherent culture dishes and cultured for 24 hr. The medium was then changed to serum-free ES cell medium supplemented with insulin (5 μg/ml), transferrin (50 μg/ml), selenium chloride (30 nM), and fibronectin (50 μg/ml) to select nestin-positive NPCs (stage 3). After 7 days of selection, nestin-positive NPCs were dissociated using 0.05% trypsin and 1 mM EDTA and plated onto coverglasses coated with poly-L-ornithine (Sigma) and 1 μg/ml laminin at a density of $1–1.5 \times 10^5$ cells/cm$^2$ in DMEM/F-12 (1 : 1) with $N_2$ supplement (Invitrogen), 20 ng/ml FGF-2 (Invitrogen), and 1 μg/ml laminin (Invitrogen) and cultured for 6 days to expand NPCs (stage 4). Differentiation of NPCs into neurons was induced by DMEM/F-12 (1:1) supplemented with $N_2$ supplement (Invitrogen), laminin (1 μg/ml), and ascorbic acid (200 μM) for 6 days (stage 5). For cell culture in low-oxygen conditions, ES cell-derived NPCs were cultured in automatic $O_2/CO_2$ incubators (Model 9200; Wakenyaku Co., Japan) at 3.5% $O_2$ plus 5% $CO_2$ with $N_2$ from stage 4 to stage 5.

### Immunocytochemistry

Cells were fixed in 4% paraformaldehyde (PFA) in PBS at room temperature (RT) for 20 min, washed, permeabilized with 0.25% Triton-X in PBS, and blocked with 3% horse serum or 10% normal goat serum. Cells were then incubated for 1 hr at RT or overnight at 4°C with the primary antibodies against mouse anti-nestin monoclonal antibody (1:500; Chemicon), mouse anti-β-tubulin III monoclonal antibody (1:500; Sigma), mouse anti-MAP-2 monoclonal antibody (1:500; Chemicon), mouse anti-TH monoclonal antibody (1:1,000; Sigma), rabbit anti-glial fibrillary acidic protein (GFAP) polyclonal antibody (1:500; Dako A/S, Glostrup, Denmark). After three washes with 0.25% Triton-X in PBS, cells were visualized with fluorescein isothiocyanate (FITC)-conjugated goat anti-mouse, rhodamine-conjugated goat anti-rabbit IgG antibody (1:1,000; Molecular Probes, Eugene, OR), or with biotinylated horse anti-mouse IgG followed by a Vector ABC kit with DAB reaction.

### Western Blot

Cells were washed with PBS and were first lysed with buffer A [20 mM HEPES, 10 mM KCl, 1 mM EDTA, 1 mM dithiothreitol (DTT), 0.2% Triton X-100, 10% glycerol, 1 mM phenylmethylsulfonyl fluoride (PMSF), and 1 μg/ml protease inhibitor cocktail]. The proteins were incubated on ice for 5 min and then centrifuged at 13,000*g* at 4°C for 10 min. The supernatant was obtained (cytosolic protein extracts) and stored at −80°C.

The pellet was lysed with buffer B (350 mM NaCl, 20% glycerol, 20 mM HEPES, 10 mM KCl, 1 mM EDTA, 1 mM PMSF, and 1 μg/ml protease inhibitor), mixed vigorously by vortexing, and then incubated on ice for 30 min. The protein was centrifuged at 13,000*g* at 4°C for 10 min (Pacary et al., 2006) and the supernatant (nuclear extracts) stored at −80°C. The total protein content was measured with the Bradford assay (Bio-Rad, Hercules, CA).

For HIF-1α protein detection, each sample was separated on an 8% polyacrylamide gel, and the proteins were transferred to a polyvinylidene difluoride (PVDF) membrane (Millipore, Billerica, MA). The membrane was blocked with 5% skimmed milk in Tris-buffered saline containing 0.05% Tween 20 (T-TBS) for 1 hr, washed in T-TBS, and then incubated with polyclonal rabbit anti-HIF-1α antibody (1 μg/ml; Chemicon; MAB 3883) overnight at 4°C.

For the detection of caspase-3 and α-tubulin, these proteins were separated on 12% sodium dodecyl sulfate (SDS)-polyacrylamide gel and transferred to a PVDF membrane. Primary antibodies were rabbit anticaspase-3 (1:600; Stressgen, Vancouver, British Columbia, Canada) and mouse anti-α-tubulin

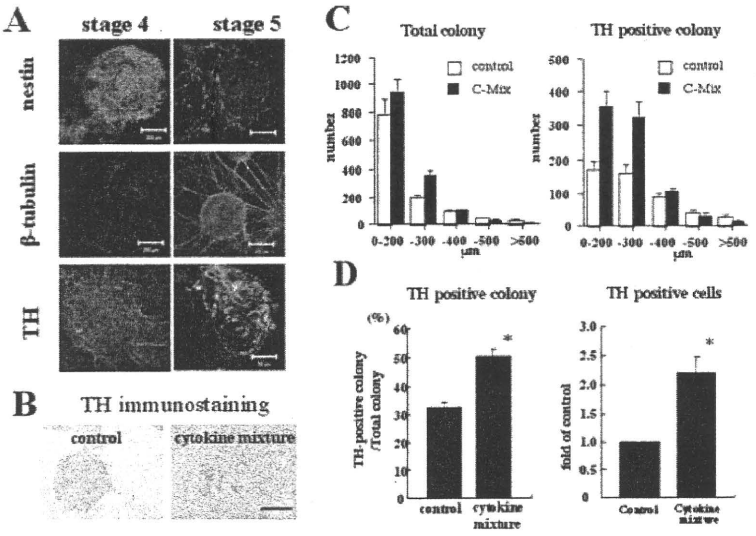


Fig. 1. Treatment with C-Mix in ES cell-derived NPCs increased TH-positive colonies and TH-positive cells. **A:** ES cells were differentiated into DAergic neurons using the five-step method. Nestin-positive NPCs (upper panel) underwent proliferation for 6 days with FGF-2 (stage 4), followed by differentiation into neurons with ascorbic acid for 6 days (stage 5). A dominant expression of nestin was found in stage 4, and most of the cells in stage 5 were β-tubulin III-positive (middle panel) and contained TH-positive cells (lower panel). **B:** Cytokine mixture (C-Mix: 200 pg/ml IL-1β, 1 ng/ml IL-11, 1 ng/ml LIF, 1 ng/ml GDNF) was applied to the NPCs every second day. TH immunostaining was carried out 6 days after differentiation. Scale bar = 100 μm. **C:** The diameter of each colony was measured and classified into one of five grades (~0–200 μm, ~200–300 μm, ~300–400 μm, ~400–500 μm, and >500 μm). There was no significant differences in the distribution patterns of the diameter in a total colony (left graph), but more TH-positive colonies in the ~0–200-μm- and ~200–300-μm-diameter groups were found after C-Mix treatment (right graph). **D:** TH-positive colonies that had more than three TH-positive cells were 32.4% ± 0.78% of total colonies, and the total number of TH-positive cells was 3,637 ± 1,053 under the control condition (n = 4). Treatment with C-Mix increased the number of TH-positive colonies (50.4% ± 2.4%, n = 4) and TH-positive cells (2.20- ± 0.29-fold of control, n = 4). $*P < 0.05$ compared with the respective controls.

(1:8,000; Sigma). After washing in T-TBS, the membrane was incubated with peroxidase-conjugated anti-mouse IgG (1:2,000; Sigma) or anti-rabbit IgG (1:5,000; Sigma) for 1 hr at RT.

Immunoreactive signals were visualized by ECL Western blotting detection reagents (Amersham Pharmacia Biotech, Arlington Heights, IL). Band intensity was analyzed in NIH Image 1.61. Ratios of the intensity of caspase-3 and HIF-1α to those of α-tubulin are presented as percentages of non-treated controls.

### Assessment of Cell Proliferation

To assess cell proliferation, nestin-positive cells cultured in 96-well plates were treated with bromodeoxyuridine (BrdU; 10 μM) for 2 hr at day 4 in stage 4. BrdU incorporated into the cells was analyzed with an ELISA kit (Amesham Pharmacia Biotech) according to the manufacturer's recommendations. The optical density (O.D.) of absorption at 450 nm was used as the data because of the linear increase of O.D. with increments of BrdU incorporation.

### Cell Count of TH-Positive Colonies and TH-Positive Cells

After cells were immunostained with TH antibody, the diameter of each colony was measured, and the numbers of TH-immunopositive cells were counted in all fields of 13-mm-diameter circular glass slides under a brightfield microscope (AX70; Olympus, Tokyo, Japan). Some colonies from ES cell-derived NPCs formed aggregates during cell expansion, causing difficulties for accurate measurement; therefore, aggregated colonies with a diameter of more than 300 μm were omitted from cell counting (see Fig. 1C).

Two parameters were used in the assessment of TH-positive colonies and cells. Because almost all single colonies were less than 300 μm, we first counted the total number of single colonies and next defined a colony in which there were more than three TH-positive cells as a TH-positive colony. The total number of TH-positive cells in a TH-positive colony was counted as the number of TH-positive cells. Slight variations in the number of TH-positive cells were found (3,637 ± 1,053 from four independent experiments) because of difficulties in constant cell plating at stage 4. Thus, data for the number of TH-positive cells are presented as the percentage of control in each experiment.

To estimate the percentage of TH-positive cells in the total cells of a colony, staining for TH, Nurr-1 (rabbit polyclonal; 1:100; Santa Cruz Biotechnology, Santa Cruz, CA), and DAPI was carried out followed by assessment using confocal microscopy. Immunofluorescent pictures of 0.65-μm-thick sections were obtained in a colony (~250 μm diameter) by confocal microscopy (Eclipse TE200-U; Nikon) for each of TH, Nurr-1, and DAPI staining. The number of total cells

**TABLE I. Primers for Real-Time PCR**

| Primer | Forward | Reverse |
|---|---|---|
| β-Tubulin III | AAGGCCTTCCTGCACTGGTA | TCTCGGCCTCGGTGAACTC |
| DBH | TTCCAATGTGCAGCTGAGTC | TATCTTCCGTGGGTTGTGGT |
| GAD67 | GCGGGAGCGGATCCTAATA | TGGTGCATCCATGGGCTAC |
| GAPDH | TGTGTCCGTCGTGGATCTGA | CCTGCTTCACCACCTTCTTGA |
| GFAP | CGCTCAATGCTGGCTTCA | AAGCGGTCATTGAGCTCCAT |
| GluTI | AGTGTATCCTGTTGCCCTTCT | CATCGGCTGTCCCTCGAAGC |
| HIF-lα | TACAGTCAGCAACGTGGAAG | TATCGAGGCTGTGTCGACTG |
| HuD | GCCTCGATCAGGGATGCTAA | GTGATGATGCGACCGTATTGA |
| Nurr-1 | GCCCGATGTGGGACGAT | TCTGCTCGATCATATGCGTAGTG |
| Oilg2 | CTGGTGTCTAGTCGCCCATC | AGGAGGTGCTGGAGGAAGAT |
| S-100β | TGCCCTCATTGATGTCTTCCA | GAGAGAGCTCGTTGTTGATGAGCT |
| TH | AGGAACGGACTGGCTTCCA | CCTGCTTCACCACCTTCTTGA |
| TPH1 | CACGAGTGCAAGCCAAGGTTT | AGTTTCCAGCCCCGACATCAG |

was counted from the DAPI nuclear staining. The numbers of TH-positive and Nurr-1-positive cells were counted from TH and Nurr-1 stainings, respectively.

### HPLC

To measure DA metabolites in the medium, an HPLC system with an electrochemical detector (HPLC-ECD-100; Eicom, Japan) was used, as reported previously (Hida et al., 1999; Jung et al., 2004), with some modifications. Briefly, 1 ml culture medium was added to 0.5 ml Tris buffer (1.5 M, pH 8.6) containing 20 μl of 0.5 M EDTA-2Na and 20 mg aluminium oxide 90 active basic (Merck), followed by gentle vortexing for 5 min. After aluminium oxide 90 had been thoroughly washed with water, adsorbed catecholamines were extracted with 120 μl of 2% acetic acid containing 100 μM EDTA. A 50-μl aliquot of each sample was injected into the HPLC-ECD system and separated with a CA-5ODS column (Eicom) with constant flow (0.5 ml/min) of the mobile phase buffer (14.9 g/liter citric acid, 1.93 g/liter sodium acetate, 110 mg/liter sodium l-octanesulfonate, 5 mg/liter EDTA, 15% methanol at pH 2.6). The peak times for noradrenalin (NA), L-dopa, DOPAC, and DA were 4.4, 5.7, 6.2, and 7.7 min, respectively.

### Inhibition of HIF-1α Expression by Treatment With Antisense Oligodeoxynucleotides (ODNs)

To suppress HIF-1α expression, phosphorothioate antisense ODNs (5′-CCTCCATGGCGAATCGGTGC-3′) or scrambled ODNs (5′-ACTCGTACCGCGGCAGTTCG-3′) were synthesized as previously reported (Yang et al., 2005). HIF-1α antisense ODNs or scrambled ODNs (50 μM) were added to cells at the time of plating (during stages 4 and 5) and were present during the culture, as previously reported (Florez-McClure et al., 2004).

### Real-Time Measurement of PCR

Total RNA from cells was isolated with Trizol reagent (Gibco/Invitrogen), and PCR was carried out with qPCR MasterMix Plus for Sybr Green (Eurogentec, San Diego, CA) with a manual procedure: incubation at 95°C for 10 min, followed by 40 cycles of amplification (15 sec at 95°C, 1 min at 60°C, 45 sec at 72°C, and 15 sec at 80°C) for Sybr Green detection. For measurement of HIF-1α, 45 cycle amplification (15 sec at 95°C, 1 min at 57°C, 45 sec at 72°C, and 15 sec at 80°C) was used. The primers used for real-time measurement of PCR are summarized in Table I.

The expression of each gene was normalized by the corresponding amount of *GAPDH* mRNA. The relative amounts of each product were calculated using the comparative $CT^{2^{-\Delta\Delta CT}}$ method described in User Bulletin No. 2 of the ABI Prism 7000 Sequence Detection System (Applied Biosystems, Foster City, CA).

## RESULTS

### Treatment With Cytokine Mixture (C-Mix) in ES Cell-Derived NPCs Induced Into DAergic Neuron Differentiation

ES cells were induced to differentiate into DAergic neurons by using the five-step method. A dominant expression of nestin was found in stage 4 (Fig. 1A), and most cells differentiated into β-tubulin III-positive and partially TH-positive cells (Fig. 1A). Microtubule-associated protein-2 (MAP-2)-positive neurons, GFAP-positive astrocytes, and O1-positive oligodendrocytes were also seen in stage 5 (data not shown). Because accurate measurements of the numbers of TH-positive and total cells were difficult in our method because of cell aggregations, colonies with a diameter of less than 300 μm were counted with two parameters: total number of single and TH-positive colonies with more than three TH-positive cells. After differentiation, TH-positive colonies that had more than three TH-positive cells were 32.4% ± 0.78% (n = 4) of the total colonies, and the total number of TH-positive cells was 3,637 ± 1,053 (n = 4) under control conditions. To assess the percentage of TH-positive cells in total cells, semiquantitative assessment was carried out from 10 representative sections of a colony by using confocal microscopy. TH-positive cells among total cells (557.9 ± 16.4, n = 10) were 2.29% ± 0.33% (n = 10), and Nurr-1-positive cells were 3.04% ± 0.65% (n = 10) in nontreated controls in our culture.

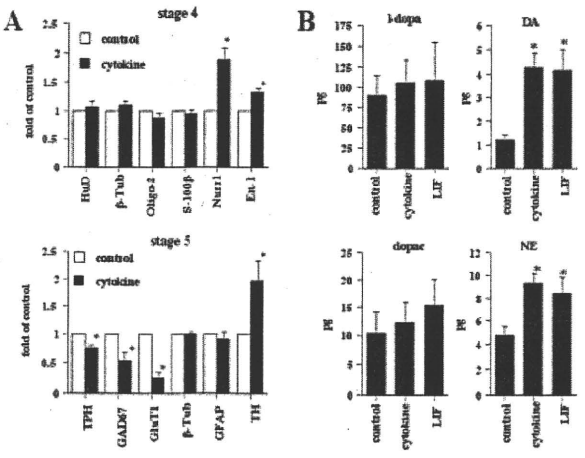


Fig. 2. Treatment with C-Mix induced gene expression of DAergic markers and DA production. **A:** Gene expressions of neural markers (HuD, β-tubulin III, Olig-2, S-100β, Nurr-1, En-1, TPH, GAD67, GluT1, GFAP, TH) were investigated in stage 4 (upper graph) and stage 5 (lower graph) in C-Mix-treatment. Expressions of Nurr-1 and En-1 mRNA were enhanced in NPCs, although the expressions of HuD, β-tubulin III, Olig-2, and S-100β mRNA were not significantly changed. TH mRNA increased in cytokine mixture-treated cells, whereas GluT1, TPH, and GAD67 were significantly decreased by C-Mix treatment. **B:** The contents of L-dopa, DA, DOPAC, and NE in the medium were measured by HPLC after C-Mix treatment. The volumes of DA and NE were increased by the treatment, but there was no difference in the contents of L-dopa and DOPAC between those with C-Mix treatment and controls.

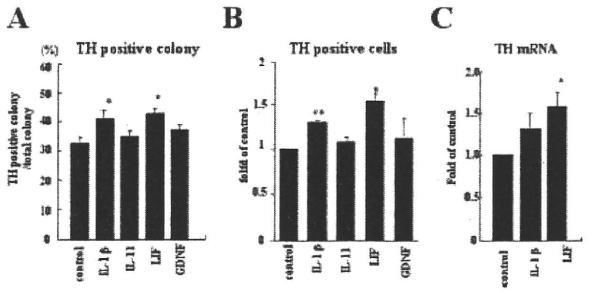


Fig. 3. Treatment with LIF or IL-1β enhanced the generation of DAergic neurons. ES cell-derived NPCs were treated with IL-1β (200 pg/ml), IL-11(1 ng/ml), LIF (1 ng/ml), or GDNF (1 ng/ml), and the number of TH-positive cells and the expression of TH mRNA after differentiation (day 6 in stage 5) were then investigated. **A:** The number of TH-positive colonies was counted and is presented as the percentage of the total colony (n = 4). LIF treatment significantly increased the number of TH-positive colonies (control: 32.4% ± 2.0% of total colonies, LIF: 42.9% ± 1.9%). **B:** The number of TH-positive cells was counted (n = 4). LIF treatment significantly increased the number of TH-positive cells (1.54- ± 0.09-fold), as did IL-1β treatment (1.31- ± 0.02-fold). **C:** Enhanced expression of TH mRNA was found with LIF treatment compared with control (1.58- ± 0.16-fold of control, n = 8).

To investigate whether C-Mix (200 pg/ml IL-1β, 1 ng/ml IL-11, 1 ng/ml LIF, 1 ng/ml GDNF) induced DAergic differentiation, ES cell-derived NPCs were treated with C-Mix (Fig. 1B). Treatment with C-Mix increased the number of TH-positive colonies (50.4% ± 2.4% of total colonies) and TH-positive cells (2.20- ± 0.29-fold of control: 8,234 ± 2,689 cells, n = 4) compared with nontreated controls (Fig. 1D). Semiquantitative assessment of the percentage of TH-positive cells among total cells showed that it was 5.54% ± 1.08% (n = 10) of total cells (560.9 ± 12.0, n = 10) in C-Mix treatment, which was significantly greater than in controls ($P < 0.05$). The percentage of Nurr-1-positive cells was 6.56% ± 1.72% (n = 10) of total cells.

Treatment with C-Mix did not increase the size of the colonies (Fig. 1C). This was confirmed by bromodeoxyuridine (BrdU) incorporation experiments: a similar level of BrdU incorporation was detected in C-Mix treated-NPCs (O.D.: 0.75 ± 0.03, n = 3) and in nontreated controls (O.D.: 0.65 ± 0.13, n = 5). Expression of Nurr-1 and En-1 mRNA (day 4 in stage 4) was enhanced in NPCs treated with C-Mix compared with nontreated controls (1.90- ± 0.18- and 1.33- ± 0.07-fold of control, respectively), although the expressions of HuD, β-tubulin III, Olig-2, and S-100β mRNA were not significantly changed (Fig. 2A, upper graph).

To determine the phenotype of cells induced by C-Mix, expression of mRNA following differentiation (day 6 in stage 5) was investigated (Fig. 2A, lower graph). TH mRNA was increased in C-Mix-treated cells (1.96- ± 0.37-fold of control); however, mRNAs of β-tubulin III and GFAP were unchanged. Expression of glutamate transporter mRNA (GluT1; a glutamatergic marker, 0.25- ± 0.09-fold), tryptophan hydroxylase (TPH; a serotonergic marker, 0.74- ± 0.06-fold), and GAD67 (a GABAergic marker, 0.54- ± 0.13-fold) were significantly decreased by C-Mix treatment.

The volume of L-dopa, DA, DOPAC, and norepinephrine (NE) in the medium was investigated by HPLC following treatment with C-Mix (Fig 2B). The contents of DA and NE were 1.21 ± 0.22 pg (n = 5) and 4.74 ± 0.78 pg (n = 5), respectively, in the nontreated controls and 4.28 ± 0.61 pg (n = 5) and 9.34 ± 0.81 pg (n = 5), respectively, following C-Mix treatment. There were no differences in the contents of L-dopa and DOPAC between C-Mix treatment and nontreated controls.

Because NE was increased by C-Mix treatment, the expression of DBH mRNA was investigated by real-time PCR. There was no increase of DBH mRNA by C-Mix treatment (1.03 ± 0.16-fold of control, n = 3).

### The Major Effect of the Cytokine Mixture Is Caused by LIF and IL-1β

To investigate which component of the C-Mix was effective in NPC differentiation into DAergic neurons, ES cell-derived NPCs were treated with 200 pg/ml IL-1β, 1 ng/ml LIF, 1 ng/ml IL-11, or 1 ng/ml

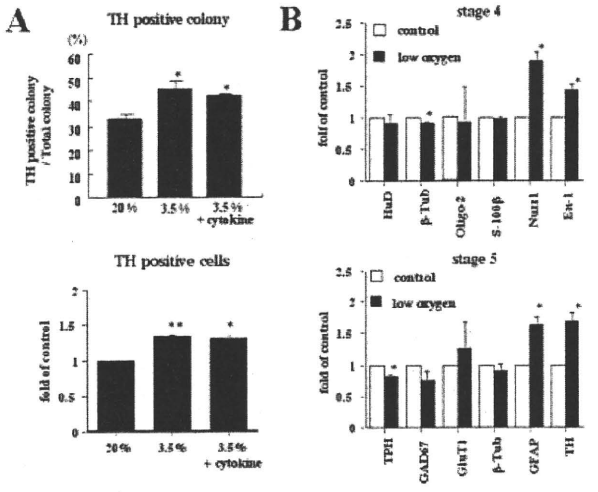


Fig. 4. Low-oxygen (L-Oxy) conditions increased the number of TH-positive cells. **A:** ES cell-derived NPCs were exposed to 3.5% $O_2$ conditions, followed by induction to neurons under L-Oxy. Exposure to L-Oxy increased the number of TH-positive colonies (3.5% $O_2$: 45.0% ± 3.6%, n = 3) and TH-positive cells (3.5% $O_2$: 1.35 ± 0.03, n = 3). When L-Oxy was combined with C-Mix, the numbers of TH-positive colonies and TH-positive cells were similar to those seen with L-Oxy alone (n = 3). $*P < 0.05$ compared with control. **B:** Gene expression of neural markers (HuD, β-tubulin III, Olig-2, S-100β, Nurr-1, En-1, TPH, GAD67, GluT1, GFAP, and TH) were investigated in stage 4 (upper graph) and stage 5 (lower graph) with L-Oxy treatment. Expressions of Nurr-1 and En-1 mRNA were enhanced in stage 4, although a slight decrease of β-tubulin III was found. TH mRNA and GFAP mRNA were increased but TPH mRNA was decreased by L-Oxy treatment.

GDNF (Fig. 3). LIF treatment significantly increased the number of TH-positive colonies (42.9% ± 1.7%, n = 5), TH-positive cells (1.54- ± 0.09-fold of control, n = 3), and expression of TH mRNA (1.58- ± 0.16-fold of control, n = 8; Fig. 3). IL-1β treatment induced NPCs differentiation into DAergic neurons (colonies: 40.9% ± 3.0%, n = 4; TH-positive cells: 1.31- ± 0.02-fold, n = 4; TH mRNA expression: 1.32- ± 0.17-fold, n = 4). However, treatment with either IL-11 or GDNF had no effect on TH-positive colonies, TH-positive cells, or expression of TH mRNA.

## No Additive Effect on NPCs Differentiation Into DAergic Neurons by C-Mix in Combination With Low Oxygen (L-Oxy)

DAergic neurons can be generated from fetal midbrain NPCs by L-Oxy levels in vitro (Studer et al., 2000). To investigate whether low physiological oxygen in the fetal brain induced DAergic differentiation of neurospheres, ES cell-derived NPCs (relatively pure NPCs compared with midbrain neurospheres) were exposed to 3.5% $O_2$, followed by neuronal differentiation under L-Oxy (Fig. 4).

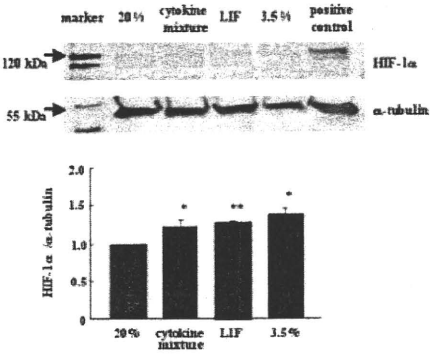


Fig. 5. HIF-1α protein was increased by C-Mix or L-Oxy. Total proteins were obtained from ES cell-derived NPCs treated with C-Mix, LIF, and low oxygen. HIF-1α (120 kDa) and α-tubulin (55 kDa) were detected by Western blot as described in Materials and Methods (upper panel). Ratios of the intensity of HIF-1α to those of α-tubulin are presented as the percentage of nontreated controls (lower panel). HIF-1α expression was increased with each treatment compared with nontreated controls. Data are shown as mean ± SE (n = 3). $*P < 0.05$, $**P < 0.001$ compared with 20% $O_2$ control. Positive control: $CoCl_2$-treated SH-SY5Y cells.

Many TH-positive cells were observed in the low 3.5% $O_2$ condition compared with the 20% $O_2$ condition (Fig. 4A), although colony size in 3.5% $O_2$ was smaller than that in 20% $O_2$. Cell culture under L-Oxy conditions caused significant increases in the numbers of TH-positive colonies (3.5% $O_2$: 45.0% ± 3.6% of total colonies, n = 3), TH-positive cells (3.5% $O_2$: 1.35- ± 0.03-fold of 20% control, n = 3; Fig 4A), and TH mRNA expression (1.68- ± 0.17-fold of control). During L-Oxy exposure, mRNA expression of Nurr-1 and En-1 in NPCs (day 4 in stage 4) was increased compared with nontreated controls (1.90- ± 0.12-fold of control and 1.43- ± 0.10-fold, respectively; Fig 4B, upper graph). Although the expression of β-tubulin III was decreased by L-Oxy, expressions of HuD, Olig-2, and S-100β mRNA were not significantly changed (Fig 4B, upper graph).

To investigate the phenotype of cells induced by L-Oxy, the expression of mRNA following differentiation (day 6 in stage 5) was investigated (Fig 4B, lower graph). Significant increases in TH mRNA (1.68- ± 0.14-fold of control) and GFAP mRNA (1.63- ± 0.13-fold) were found under L-Oxy conditions; however, a slight decrease in the mRNA expression of TPH (0.81- ± 0.05-fold) was also found (Fig 4C, lower graph). No changes were found in the mRNA expression of GluT1 or β-tubulin III. With a combination of C-Mix and L-Oxy, the numbers of TH-positive colonies (42.6% ± 0.76% of total colonies) and TH-positive cells (1.32 ± 0.03, n = 3) were not significantly increased compared with those under the 3.5% $O_2$ condition alone (Fig. 4A).

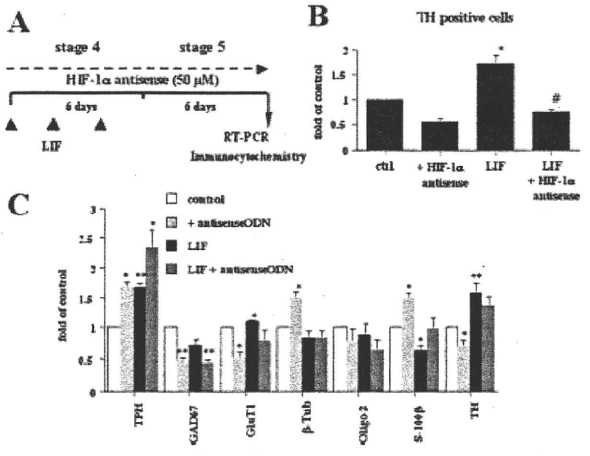


Fig. 6. Inhibition of HIF-1α proteins caused a decrease in the generation of TH-positive cells. **A:** Protocol for inhibition of endogenous and inducible HIF-1α proteins. Antisense ODNs (50 μM) for HIF-1α were applied to NPCs (stage 4) and differentiating neurons (stage 5). TH immunostaining and real-time PCR were carried out 6 days after differentiation. **B:** Treatment with antisense ODNs alone caused a decrease in the number of TH-positive cells (0.54- ± 0.07-fold of control; n = 3), but there was no significant decrease in TH-positive colonies (control: 31.4% ± 4.3%, antisense ODNs: 28.7% ± 4.4%, n = 3). The LIF-mediated increase of TH-positive cells was blocked by HIF-1α inhibition (LIF: 1.71- ± 0.19-fold of control, n = 3; LIF + antisense ODNs: 0.76 ± 0.04, n = 3). $*P < 0.05$ compared with 20% $O_2$ control, $^{\#}P < 0.05$ for comparison between LIF and LIF + antisense ODNs. **C:** Gene expressions of neural markers (TPH, GAD67, GluT1, β-tubulin III, Olig-2, S-100β, TH) were investigated in stage 5. Gene expressions of TH, GAD67, and GluT1 were decreased, and those of TPH, β-tubulin III, and S-100β were increased by ODNs treatment alone, indicating the important endogenous effect of HIF-1α in neuronal differentiation. However, no decrease in TH mRNA was noted with scrambled ODNs treatment (n = 3). TPH expression was induced by LIF alone, and the expression was further enhanced by the addition of antisense ODNs (LIF: 1.68- ± 0.07-fold, LIF plus antisense ODNs: 2.34- ± 0.29-fold, n = 3). $*P < 0.05$, $**P < 0.01$ compared with 20% $O_2$ control.

### No Activation of Caspase-3 by Cytokine Mixture and Low Oxygen

Activation of caspase-3 was investigated by using Western blot analysis for caspase-3 protein. Although both the active form (20 and 18 kDa) and the inactive form (36 kDa) of caspase-3 were detected in HeLa cell lysate, no apparent activation of caspase-3 (band of 20 and 18 kDa) was shown in ES cell-derived NPCs exposed to C-Mix, LIF, or L-Oxy (data not shown).

### Effect of HIF-1α on NPCs Differentiation Into DAergic Neurons

The effect of C-Mix on DAergic differentiation was found not to be additive to that of L-Oxy, so we focused our attention on the effect of HIF-1α. To investigate whether HIF-1α protein was increased by treatment with C-Mix, we carried out Western blot analysis for HIF-1α protein (Fig. 5). HIF-1α protein was increased following C-Mix-treatment (1.24- ± 0.07-fold of control), LIF treatment (1.29- ± 0.01-fold), and L-Oxy treatment (1.40- ± 0.07-fold). Quantitative measurements by real-time PCR revealed that the expression of HIF-1α mRNA was enhanced by treatment of C-Mix (1.94 ± 0.09, n = 3; $P < 0.01$), LIF alone (1.83 ± 0.07, n = 3; $P < 0.01$), and L-Oxy (1.92 ± 0.23, n = 4; $P < 0.05$).

To examine whether the inhibition of HIF-1α expression caused the attenuation of ES cell-derived NPCs differentiation into DAergic neurons, cells (from stages 4 and 5) were treated with HIF-1α antisense ODNs (50 μM), followed by detection of TH-positive colonies, TH-positive cells, and TH mRNA (Fig. 6). Our preliminary data showed that the addition of HIF-1α antisense ODNs (50 μM) effectively decreased the expression of HIF-1α mRNA (control + antisense: 0.59- ± 0.04-fold of control, n = 3; $P < 0.05$), although that of HIF-1α scramble ODNs (50 μM) did not change the expression (0.98 ± 0.09, n = 2). Treatment with antisense ODNs alone caused a decrease in the number of TH-positive cells (0.54- ± 0.07-fold of control, n = 3; Fig. 6B) and the expression of TH mRNA (0.70- ± 0.09-fold of control, n = 5; Fig. 6C), whereas there was no significant decrease in the TH-positive colonies observed (control: 31.4% ± 4.3%, antisense ODNs: 28.7% ± 4.4%, n = 3). When HIF-1α expression was inhibited, LIF-mediated NPC differentiation into DAergic neurons was blocked: the increase in the number of TH-positive cells was attenuated by treatment with HIF-1α antisense ODNs (LIF: 1.71- ± 0.19-fold of control, LIF plus antisense ODNs: 0.76- ± 0.04-fold of control), although the number of TH-positive colonies did not change (LIF: 39.3% ± 2.3%, LIF plus antisense ODNs: 37.6% ± 4.1%, n = 3).

Expression of mRNA following differentiation was investigated by HIF-1α antisense ODNs treatment (Fig. 6C). Significant increases in TPH mRNA (1.68- ± 0.07-fold of control, n = 3), S-100β (1.49- ± 0.09-fold, n = 3), and β-tubulin III mRNA (1.49- ± 0.10-fold, n = 3) were found after antisense ODNs treatment alone, but decreases were found in GAD67 (0.47- ± 0.05-fold, n = 3) and GluT1 (0.51- ± 0.10-fold, n = 3). Although TPH expression was induced by LIF alone, the expression was enhanced by the addition of antisense ODNs (LIF: 1.68- ± 0.07-fold, LIF plus antisense ODNs: 2.34- ± 0.29-fold, n = 3).

## DISCUSSION

To enhance NPC differentiation into DAergic neurons and to understand the differentiation mechanism, we used ES cell-derived NPCs (a relatively pure population of NPCs). We focused on the application of cytokines and trophic factors that are enhanced in DA-depleted striatum and/or low physiological oxygen in fetal brain. We found that C-Mix treatment and L-Oxy

conditions induced NPCs differentiation into DAergic neurons and that this was mediated by HIF-1α.

The differentiation of ES cells into NPCs and mature neurons has been reported as possibly induced by RA treatment (Li et al., 1998), the SDIA method (Kawasaki et al., 2000), and the five-step method (Lee et al., 2000). The five-step method by the McKay group appeared to us to be the most appropriate method for understanding the mechanism of DAergic differentiation. This was because neuronal (DAergic) differentiation in ES cells is induced by a step-by-step method (Lee et al., 2000). ES cell-derived NPCs are expanded with fibroblast growth factor (FGF)-2, and most are nestin-positive NPCs (Fig. 1A; Jung et al., 2004). This means that these cells are a relatively pure population of NPCs compared with neurospheres prepared from fetal brain (Reynolds and Weiss, 1992; Gage, 1998). It was reported recently that NPCs derived from ES cells, but not those from fetal ventral mesencephalon, maintain potency to differentiate into DAergic neurons after expansion (Chung et al., 2006). We reported that DAergic differentiation of ES cell-derived NPCs was enhanced by treatment with the trophic factor pleiotrophin (PTN), which was highly expressed in neurospheres (Jung et al., 2004) and is enhanced in DA-depleted striatum (Hida et al., 2003).

Although treatment of a cytokine mixture (IL-1β, IL-11, LIF, and GDNF) in lineage-restricted mesencephalic NPCs increased DAergic neurons (Ling et al., 1998; Potter et al., 1999; Carvey et al., 2001; Storch et al., 2001), the mechanism involved in the differentiation of NPCs into DAergic neurons remains unclear. We reported that the expressions of IL-1β, IL-11, LIF, and GDNF mRNA were increased in DA-depleted striatum (Hida et al., 2003), so we first investigated whether treatment with C-Mix increased DAergic neurons from ES cell-derived NPCs. We determined that DAergic neurons (TH-positive colonies and TH-positive cells) were increased by treatment with C-Mix and that most of this effect was caused by LIF or IL-1β treatment alone. Specific enhancement of Nurr-1 and En-1 mRNA in NPCs and TH mRNA following differentiation in the presence of C-Mix strongly supports the idea that ES cell-derived NPC differentiation into DAergic neurons was induced by C-Mix. However, we could not rule out the possibility that C-Mix specifically prevented cell death of DAergic progenitors, in that it has been reported that Nurr-1 is a survival factor for late DAergic precursors (Saucedo-Cardenas et al., 1998). However, activation of caspase-3 was not detected in our experiment.

Other studies have reported that L-Oxy conditions enhance neurogenesis and DAergic differentiation in mesencephalic NPCs (Studer et al., 2000). Similar results were observed in this study: enhanced differentiation of ES cell-derived NPCs into DAergic neurons was shown under 3.5% oxygen conditions. Contrary to the effect of L-Oxy in stage 4, in our preliminary data, a decrease in TH-positive cells was found when L-Oxy was given to embryoid bodies (EBs; stage 2) to stage 5, indicating that low-oxygen conditions act positively, not on EBs but on NPCs differentiation into DAergic neurons.

There was no additive effect from the combination of L-Oxy with C-Mix, suggesting that a common signal for DAergic neuron differentiation might, at least in part, be activated by L-Oxy and C-Mix (LIF or IL-1β). Because the differentiation mechanism was activated by low oxygen, and hypoxia is known to regulate the activity of TH gene transcription (Czyzyk-Krzeska et al., 1992, 1994, 1996, 1997; Norris and Millhorn, 1995; Beitner-Johnson and Millhorn, 1998; Kroll et al., 1999; Schnell et al., 2003; Leclere et al., 2004), we focused our attention on the HIF-1α transcription factor.

HIF-1α in neural cells is essential for normal development of the brain (Tomita et al., 2003). Although transcription and synthesis of HIF-1β are not affected by oxygen changes, HIF-1α proteins are rapidly degraded, resulting in essentially no detectable level of HIF-1α (Semenza, 1999; Wenger, 2002). We have shown that HIF-1α protein was increased by C-Mix treatment and L-Oxy conditions. Insofar as IL-6 is responsible for neuronal differentiation of PC12 cells induced by $CoCl_2$ (Kotake-Nara et al., 2005), and HIF-1α protein could be induced by $CoCl_2$ (Berchner-Pfannschmidt et al., 2004; Yang et al., 2005; Pacary et al., 2006), it is most likely that the enhancement of HIF-1α protein was induced in ES cell-derived NPCs by LIF treatment (an IL-6 family protein). That inhibition of HIF-1α by the application of antisense ODNs caused a decrease in the number of DAergic neurons strongly indicated that HIF-1α is involved in DAergic differentiation in NPCs. It was recently reported that DAergic differentiation in HIF-1α conditional knockout mice is markedly decreased (Milosevic et al., 2007).

It is notable that the expression of a serotonergic marker, TPH, was significantly increased in HIF-1α antisense ODNs treatment only, suggesting that endogenous HIF-1α induces DAergic differentiation from a relationship to serotonergic differentiation. From the viewpoint of mesencephalic development, the generation of DAergic neurons and of serotonergic neurons is similar in an anatomical aspect (around the isthmus) and in their demand for trophic factors (FGF-8 and sonic hedgehog; Jung et al., 2004). It is possible that in normal development mesencephalic DAergic neuron production is more dependent on HIF-1α compared with serotonergic neurons. Therefore, switching to the expression of TPH mRNA from TH mRNA in antisense ODN-treated NPCs suggests that a mesencephalic dorsal trophic factor for DAergic differentiation (PTN) might cause an increase in HIF-1α expression in NPCs. In our preliminary data, antisense ODN treatment in ES cell-derived NPCs inhibited TH mRNA expression in the presence of PTN, although PTN increased the generation of DAergic neurons in NPCs (Jung et al., 2004).

In summary, the differentiation of ES cell-derived NPCs (a relatively pure population of NPCs) into

DAergic neurons was induced by the application of C-Mix. This differentiation, which was enhanced in DA-depleted striatum and under low physiological oxygen in fetal brain, was mediated by HIF-1α.

## ACKNOWLEDGMENTS

This work was supported by Special Coordination Funds for Promoting Science and Technology (No. 13073-2125-14 to H.N. and H.H.), a Grant-in-Aid for Scientific Research (No. 15200026 to H.N.) from the Ministry of Education, Culture, Sports, Science and Technology (MECSST) of the Japanese Government and Research Grants (Nos. 14780581 and 16500203 to H.H.) from the Japan Society for the Promotion of Science (JSPS).

## REFERENCES

Arenas E. 2002. Stem cells in the treatment of Parkinson's disease. Brain Res Bull 57:795–808.

Bain G, Kitchens D, Yao M, Huettner JE, Gottlieb DI. 1995. Embryonic stem cells express neuronal properties in vitro. Dev Biol 168:342–357.

Beck KD, Valverde J, Alexi T, Poulsen K, Moffat B, Vandlen RA, Rosenthal A, Hefti F. 1995. Mesencephalic dopaminergic neurons protected by GDNF from axotomy-induced degeneration in the adult brain. Nature 373:339–341.

Beitner-Johnson D, Millhorn DE. 1998. Hypoxia induces phosphorylation of the cyclic AMP response element-binding protein by a novel signaling mechanism. J Biol Chem 273:19834–19839.

Berchner-Pfannschmidt U, Petrat F, Doege K, Trinidad B, Freitag P, Metzen E, de Groot H, Carvey PM, Ling ZD, Sortwell CE, Pitzer MR, McGuire SO, Storch A, Collier TJ. 2001. A clonal line of mesencephalic progenitor cells converted to dopamine neurons by hematopoietic cytokines: a source of cells for transplantation in Parkinson's disease. Exp Neurol 171:98–108.

Castilho RF, Hansson O, Brundin P. 2000. Improving the survival of grafted embryonic dopamine neurons in rodent models of Parkinson's disease. Prog Brain Res 127:203–231.

Chung S, Shin BS, Hwang M, Lardaro T, Kang UJ, Isacson O, Kim KS. 2006. Neural precursors derived from embryonic stem cells, but not those from fetal ventral mesencephalon, mainteain the potencial to differentiate into dopaminergic neurons after expansion in vitro. Stem Cells 24:1583–1593.

Czyzyk-Krzeska MF, Bayliss DA, Lawson EE, Millhorn DE. 1992. Regulation of tyrosine hydroxylase gene expression in the rat carotid body by hypoxia. J Neurochem 58:1538–1546.

Czyzyk-Krzeska MF, Furnari BA, Lawson EE, Millhorn DE. 1994. Hypoxia increases rate of transcription and stability of tyrosine hydroxylase mRNA in pheochromocytoma (PC 12) cells. J Biol Chem 269:760–764.

Czyzyk-Krzeska MF, Paulding WR, Lipski J, Beresh JE, Kroll SL. 1996. Regulation of tyrosine hydroxylase mRNA stability by oxygen in PC12 cells. Adv Exp Med Biol 410:143–150.

Czyzyk-Krzeska MF, Paulding WR, Beresh JE, Kroll SL. 1997. Post-transcriptional regulation of tyrosine hydroxylase gene expression by oxygen in PC12 cells. Kidney Int 51:585–590.

Dunnett SB, Bjorklund A. 1999. Prospects for new restorative and neuroprotective treatments in Parkinson's disease. Nature 399:A32–A39.

Farkas LM, Dunker N, Roussa E, Unsicker K, Krieglstein K. 2003. Transforming growth factor-beta(s) are essential for the development of midbrain dopaminergic neurons in vitro and in vivo. J Neurosci 23:5178–5186.

Florez-McClure ML, Linseman DA, Chu CT, Barker PA, Bouchard RJ, Le SS, Laessig TA, Heidenreich KA. 2004. The p75 neurotrophin receptor can induce autophagy and death of cerebellar Purkinje neurons. J Neurosci 24:4498–4509.

Gage FH. 1998. Stem cells of the central nervous system. Curr Opin Neurobiol 8:671–676.

Hida H, Hashimoto M, Fujimoto I, Nakajima K, Shimano Y, Nagatsu T, Mikoshiba K, Nishino H. 1999. Dopa-producing astrocytes generated by adenoviral transduction of human tyrosine hydroxylase gene: in vitro study and transplantation to hemiparkinsonian model rats. Neurosci Res 35:101–112.

Hida H, Jung CG, Wu CZ, Kim HJ, Kodama Y, Masuda T, Nishino H. 2003. Pleiotrophin exhibits a trophic effect on survival of dopaminergic neurons in vitro. Eur J Neurosci 17:2127–2134.

Jung CG, Hida H, Nakahira K, Ikenaka K, Kim HJ, Nishino H. 2004. Pleiotrophin mRNA is highly expressed in neural stem (progenitor) cells of mouse ventral mesencephalon and the product promotes production of dopaminergic neurons from embryonic stem cell-derived nestin-positive cells. FASEB J 18:1237–1239.

Kawasaki H, Mizuseki K, Nishikawa S, Kaneko S, Kuwana Y, Nakanishi S, Nishikawa SI, Sasai Y. 2000. Induction of midbrain dopaminergic neurons from ES cells by stromal cell-derived inducing activity. Neuron 28:31–40.

Kotake-Nara E, Takizawa S, Quan J, Wang H, Saida K. 2005. Cobalt chloride induces neurite outgrowth in rat pheochromocytoma PC-12 cells through regulation of endothelin-2/vasoactive intestinal contractor. J Neurosci Res 81:563–571.

Kroll SL, Paulding WR, Schnell PO, Barton MC, Conaway JW, Conaway RC, Czyzyk-Krzeska MF. 1999. von Hippel-Lindau protein induces hypoxia-regulated arrest of tyrosine hydroxylase transcript elongation in pheochromocytoma cells. J Biol Chem 274:30109–30114.

Leclere N, Andreeva N, Fuchs J, Kietzmann T, Gross J. 2004. Hypoxia-induced long-term increase of dopamine and tyrosine hydroxylase mRNA levels. Prague Med Rep 105:291–300.

Lee SH, Lumelsky N, Studer L, Auerbach JM, McKay RD. 2000a. Efficient generation of midbrain and hindbrain neurons from mouse embryonic stem cells. Nat Biotechnol 18:675–679.

Li M, Pevny L, Lovell-Badge R, Smith A. 1998. Generation of purified neural precursors from embryonic stem cells by lineage selection. Curr Biol 8:971–974.

Lindvall O. 2003. Stem cells for cell therapy in Parkinson's disease. Pharmacol Res 47:279–287.

Ling ZD, Potter ED, Lipton JW, Carvey PM. 1998. Differentiation of mesencephalic progenitor cells into dopaminergic neurons by cytokines. Exp Neurol 149:411–423.

Milosevic J, Schwarz SC, Krohn K, Poppe M, Storch A, Schwarz J. 2005. Low atmospheric oxygen avoids maturation, senescence and cell death of murine mesencephalic neural precursors. J Neurochem 92:718–729.

Milosevic J, Maisel M, Wegner F, Leuchtenberger J, Wenger RH, Gerlach M, Storch A, Schwarz J. 2007. Lack of hypoxia-inducible factor-1 alpha impairs midbrain neural precursor cells involving vascular endothelial growth factor signaling. J Neurosci 27:412–421.

Nishino H, Hida H, Takei N, Kumazaki M, Nakajima K, Baba H. 2000. Mesencephalic neural stem (progenitor) cells develop to dopaminergic neurons more strongly in dopamine-depleted striatum than in intact striatum. Exp Neurol 164:209–214.

Norris ML, Millhorn DE. 1995. Hypoxia-induced protein binding to $O_2$-responsive sequences on the tyrosine hydroxylase gene. J Biol Chem 270:23774–23779.

Pacary E, Legros H, Valable S, Duchatelle P, Lecocq M, Petit E, Nicole O, Bernaudin M. 2006. Synergistic effects of $CoCl_2$ and ROCK inhi-

bition on mesenchymal stem cell differentiation into neuron-like cells. J Cell Sci 119:2667–2678.

Potter ED, Ling ZD, Carvey PM. 1999. Cytokine-induced conversion of mesencephalic-derived progenitor cells into dopamine neurons. Cell Tissue Res 296:235–246.

Reynolds BA, Weiss S. 1992. Generation of neurons and astrocytes from isolated cells of the adult mammalian central nervous system. Science 255:1707–1710.

Sanchez-Pernaute R, Studer L, Bankiewicz KS, Major EO, McKay RD. 2001. In vitro generation and transplantation of precursor-derived human dopamine neurons. J Neurosci Res 65:284–288.

Saucedo-Cardenas O, Quintana-Hau JD, Le WD, Smidt MP, Cox JJ, De Mayo F, Burbach JP, Conneely OM. 1998. Nurr1 is essential for the induction of the dopaminergic phenotype and the survival of ventral mesencephalic late dopaminergic precursor neurons. Proc Natl Acad Sci U S A 95:4013–4018.

Schnell PO, Ignacak ML, Bauer AL, Striet JB, Paulding WR, Czyzyk-Krzeska MF. 2003. Regulation of tyrosine hydroxylase promoter activity by the von Hippel-Lindau tumor suppressor protein and hypoxia-inducible transcription factors. J Neurochem 85:483–491.

Semenza GL. 1999. Regulation of mammalian $O_2$ homeostasis by hypoxia-inducible factor 1. Annu Rev Cell Dev Biol 15:551–578.

Semenza GL. 2003. Targeting HIF-1 for cancer therapy. Nat Rev Cancer 3:721–732.

Storch A, Paul G, Csete M, Boehm BO, Carvey PM, Kupsch A, Schwarz J. 2001. Long-term proliferation and dopaminergic differentiation of human mesencephalic neural precursor cells. Exp Neurol 170:317–325.

Studer L, Tabar V, McKay RD. 1998. Transplantation of expanded mesencephalic precursors leads to recovery in parkinsonian rats. Nat Neurosci 1:290–295.

Studer L, Csete M, Lee SH, Kabbani N, Walikonis J, Wold B, McKay R. 2000. Enhanced proliferation, survival, and dopaminergic differentiation of CNS precursors in lowered oxygen. J Neurosci 20:7377–7383.

Svendsen CN, Caldwell MA, Shen J, ter Borg MG, Rosser AE, Tyers P, Karmiol S, Dunnett SB. 1997. Long-term survival of human central nervous system progenitor cells transplanted into a rat model of Parkinson's disease. Exp Neurol 148:135–146.

Tomita S, Ueno M, Sakamoto M, Kitahama Y, Ueki M, Maekawa N, Sakamoto H, Gassmann M, Kageyama R, Ueda N, Gonzalez FJ, Takahama Y. 2003. Defective brain development in mice lacking the Hif-1alpha gene in neural cells. Mol Cell Biol 23:6739–6749.

Wenger RH. 2002. Cellular adaptation to hypoxia: $O_2$-sensing protein hydroxylases, hypoxia-inducible transcription factors, and $O_2$-regulated gene expression. FASEB J 16:1151–1162.

Yang M, Stull ND, Berk MA, Snyder EY, Iacovitti L. 2002. Neural stem cells spontaneously express dopaminergic traits after transplantation into the intact or 6-hydroxydopamine-lesioned rat. Exp Neurol 177:50–60.

Yang YT, Ju TC, Yang DI. 2005. Induction of hypoxia inducible factor-1 attenuates metabolic insults induced by 3-nitropropionic acid in rat C6 glioma cells. J Neurochem 93:513–525.

# Targeting of Myelin Protein Zero in a Spontaneous Autoimmune Polyneuropathy[1]

**Hye-Jung Kim,[2] Cha-Gyun Jung,[2] Mark A. Jensen, Danuta Dukala, and Betty Soliven[3]**

**Elimination of the costimulatory molecule B7-2 prevents autoimmune diabetes in NOD mice, but leads to the development of a spontaneous autoimmune polyneuropathy (SAP), which resembles the human disease chronic inflammatory demyelinating polyneuropathy (CIDP). In this study, we examined the immunopathogenic mechanisms in this model, including identification of SAP Ags. We found that B7-2-deficient NOD mice exhibit changes in cytokine and chemokine gene expression in spleens over time. There was an increase in IL-17 and a decrease in IL-10 transcript levels at 4 mo (preclinical phase), whereas IFN-$\gamma$ expression peaked at 8 mo (clinical phase). There was also an increase in transcript levels of Th1 cytokines, CXCL10, and RANTES in sciatic nerves of mice that developed SAP. Splenocytes from SAP mice exhibited proliferative and Th1 cytokine responses to myelin P0 (180–199), but not to other P0 peptides or P2 (53–78). Adoptive transfer of P0-reactive T cells generated from SAP mice induced neuropathy in four of six NOD.SCID mice. Data from i.v. tolerance studies indicate that myelin P0 is one of the autoantigens targeted by T cells in SAP in this model. The expression of P0 by peri-islet Schwann cells provides a potential mechanism linking islet autoimmunity and inflammatory neuropathy.** *The Journal of Immunology,* **2008, 181: 8753–8760.**

The NOD mouse spontaneously develops polyendocrine autoimmunity and is used as a model for type 1 diabetes, thyroiditis, and Sjögren's syndrome, as reviewed previously (1). Manifestations of autoimmunity in NOD mice are regulated by the cytokine milieu, and by costimulatory molecules such as B7-1 and B7-2. Neutralization or deficiency of B7-1 causes exacerbation of diabetes. In contrast, elimination of B7-2 leads to protection against diabetes, although peri-insulitis is present in some mice (2–4). Interestingly, B7-2 elimination triggers the development of a spontaneous autoimmune polyneuropathy (SAP)[4] that mimics human chronic inflammatory demyelinating polyneuropathy (CIDP) clinically, histologically and electrophysiologically, albeit not in all aspects (3). Compared with SAP, CIDP is more heterogenous with regard to disease onset, and the course can be relapsing-remitting or chronic progressive. Histologically, CIDP in humans is characterized by the presence of segmental demyelination in peripheral nerves and nerve roots, axonal loss of variable degree, and an immune-mediated pathophysiology (5). NOD mice can develop both type 1 diabetes and SAP, or exclusively one but not the other, thought to depend on the balance between effector T cells and regulatory T cells (Tregs) (6).

Based on the cytokine profile, $CD4^+$ effector T cells are classified into IFN-$\gamma$-producing Th1 cells, IL-4-producing Th2 cells, and IL-17-producing Th17 cells (7, 8). Both Th1 and Th17 cells are capable of inducing autoimmunity (9). The recruitment of effector T cells and macrophages into the target organ of autoimmunity is directed by chemokines and their receptors. For example, CXCL10 (IP-10), a chemoattractant for T cells, has been implicated in the pathogenesis of CIDP (10, 11). The goal of this study was to elucidate the molecular mechanisms underlying the pathogenesis of SAP in B7-2 knockout (KO) NOD mice, focusing on the characterization of cytokine and chemokine profile, and the identification of potential SAP Ags. Candidate SAP Ags include but are not limited to known proteins of peripheral nerve myelin such as P0, P2 that can induce experimental autoimmune neuritis (EAN), a model of human Guillain-Barré syndrome (12–15). We chose to focus on myelin protein zero (Mpz), or P0, in this study. It should be noted that $P0^{+/-}$ mice develop an inflammatory neuropathy spontaneously that is attributed to impaired central tolerance to P0 (16–18). In CIDP, proliferative responses to P0 or P2 as well as autoantibodies against P0, P2, and glycolipids have been reported in some patients (15.6–46%) but none has been shown to be highly sensitive and specific (19–21). This finding may reflect epitope spreading of variable extent or more likely the heterogeneity of this disease. Given the development of inflammatory neuropathy in NOD mice lacking B7-2, it is plausible that CIDP-like illness occurring on the background of type 1 diabetes is a unique subset characterized by autoreactivity to a specific peripheral nervous system (PNS) Ag that is shared by pancreatic islets.

## Materials and Methods

### *Clinical and electrophysiology assessment*

All animal use procedures were conducted in strict accordance to the National Institutes of Health and University of Chicago institutional guidelines. For clinical assessment, the following nominal scale was used: 0—normal; 1—flaccid tail; 2—mild paraparesis; 3—severe paraparesis; 4—tetraparesis; 5—death. Grip strength testing consisted of five separate measurements in each of two trials per session with a grip strength meter (Columbus Instruments). Results of two trials were averaged for each mouse per session. After the last grip strength measurement, electrophysiologic studies of sciatic nerves were performed as described in our previous publications (3, 22). Latency, conduction velocity, and peak-to-peak amplitudes were measured.

Department of Neurology, The University of Chicago, Chicago, IL 60637

Received for publication May 22, 2008. Accepted for publication September 30, 2008.

The costs of publication of this article were defrayed in part by the payment of page charges. This article must therefore be hereby marked *advertisement* in accordance with 18 U.S.C. Section 1734 solely to indicate this fact.

[1] This work was supported by Grant R21 NS049014 from the National Institutes of Health, by a pilot grant from the GBS/CIDP Foundation International, Miller Group Charitable Trust Fund (M. P. Miller III), and Jack Miller Center for Peripheral Neuropathy.

[2] H.-J.K. and C.-G.J. contributed equally to this work.

[3] Address correspondence and reprint requests to Dr. Betty Soliven, Department of Neurology, MC2030, The University of Chicago; 5841 South Maryland Avenue, Chicago, IL 60637. E-mail address: bsoliven@neurology.bsd.uchicago.edu

[4] Abbreviations used in this paper: SAP, spontaneous autoimmune polyneuropathy; CIDP, chronic inflammatory demyelinating polyneuropathy; PNS, peripheral nervous system; EAN, experimental autoimmune neuritis; GFAP, glial fibrillary acid protein; KO, knockout; P0, myelin protein zero; Treg, regulatory T cell; WT, wild type.

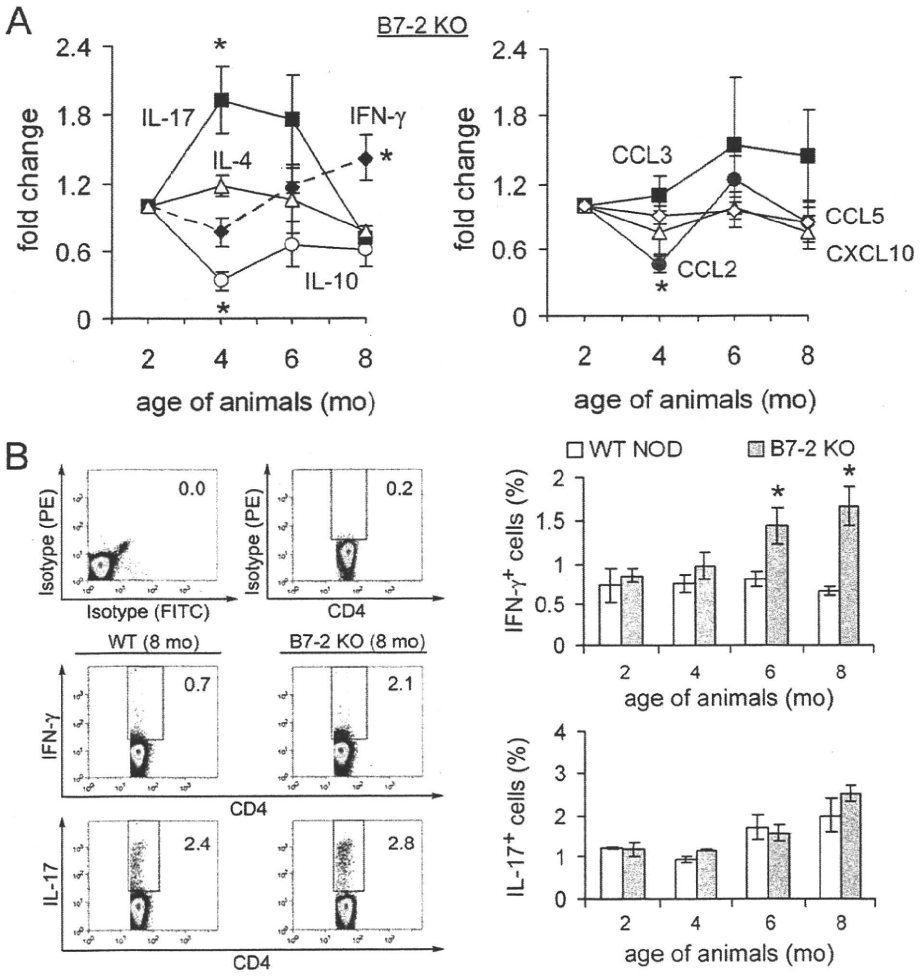


**FIGURE 1.** Cytokine and chemokine perturbations in the spleens of B7-2 KO NOD mice. *A*, Time course of cytokine and chemokine transcripts in the spleens of B7-2 KO NOD. At 4 mo (preclinical phase), there was an increase in IL-17, a decrease in IL-10 and no change in IFN-γ transcript levels. *, $p < 0.04$ for IL-17 vs IL-10; *, $p < 0.037$ for IL-17 vs IFN-γ; *, $p < 0.002$ for IL-10 vs IFN-γ. At 8 mo (clinical phase), there was evidence for Th1 bias. *, $p < 0.003$ for IFN-γ vs IL-17 and *, $p < 0.01$ for IFN-γ vs IL-10. There was a decrease in CCL2 transcript levels at 4 mo. *, $p < 0.004$ for CCL2 vs CCL3. Data shown represent an average from three independent experiments. The relative amount of each product was calculated by the threshold cycle method ($C_T = 2^{-\Delta\Delta CT}$). Data were normalized to that of 2-mo-old B7-2 KO NOD mice. *B*, Examples of intracellular cytokine analysis (*left*) and summary (*right*) showing an increase in IFN-γ-producing, but not in IL-17-producing $CD4^+$ T cells in spleens of 6- and 8-mo-old B7-2 KO mice when compared with age-matched WT NOD mice ($n = 3$ each). *, $p < 0.026$ in 8-mo data for $CD4^+$ IFN-$\gamma^+$ T cells and *, $p < 0.036$ for 6-mo data, B7-2 KO vs WT NOD. Splenocytes were incubated with PMA (10 ng/ml) and ionomycin (500 ng/ml) for 4 h.

### *Histologic studies of sciatic nerves*

Segments of the sciatic nerves were fixed in 0.5–4% paraformaldehyde, embedded in OCT compound, and snap frozen. Longitudinal sections (10 μm slices) of sciatic nerves were stained with H&E for evaluation of mononuclear cell infiltration, and used for immunohistochemistry with rat anti-CD3 Ab (1/100; Southern Biotechnology Associates) using the peroxidase method.

### *Splenocyte culture, proliferation, and cytokine production assays*

For proliferation assay, splenocytes were cultured at a density of $5 \times 10^5$ cells/well in HL-1 medium plus nonessential amino acids (BioWhittaker), 2 mM L-glutamine, 1 mM sodium pyruvate, 55 μM 2-ME in flat-bottom 96-well plates. Cells were then stimulated with Con A (2.5 μg/ml), PNS myelin (100 μg/ml), P0 peptide (20 μg/ml), P2 peptide (20 μg/ml), or Schwann cell lysates (100 μg/ml). On day 3, these cultures were pulsed for 16 h with 1 μCi [*methyl*-$^3$H]thymidine, and then harvested on glass fiber filter. The amount of incorporated [*methyl*-$^3$H]thymidine was measured using Beckman liquid scintillation counter. A stimulation index was defined by cpm in the presence of Ag divided by cpm in the absence of the Ag. Supernatants collected at 48 h from replicate cultures were assayed for IFN-γ (Endogen), IL-2, IL-10 (BD Biosciences), and IL-17 (eBioscience) using ELISA Minikits following the manufacturer's instructions. The binding of peroxidase-conjugated secondary Ab was detected by TMB Substrate Reagent set (BD Biosciences).

Ags used in in vitro T cells activation include P0 and P2 peptides, which were synthesized at the University of Chicago Protein-Peptide Core Facility. The following peptides were used: P0 (180–199) SSKRGRQTPVLY AMLDHSRS; P0 (41–60) PEGGRDAISIFHYAKGQPYI; P0 (106–125) IVGKTSQVTLYVFEKVPTRY; P2 (53–78) TESPFKNTEISFKLGQEFEE TTADNR; OVA (323–339) ISQAVHAAHAEINEAGR (GenScript). Myelin was prepared from mouse sciatic nerves as described by other investigators (23, 24). Schwann cell lysates were prepared by five cycles of rapid

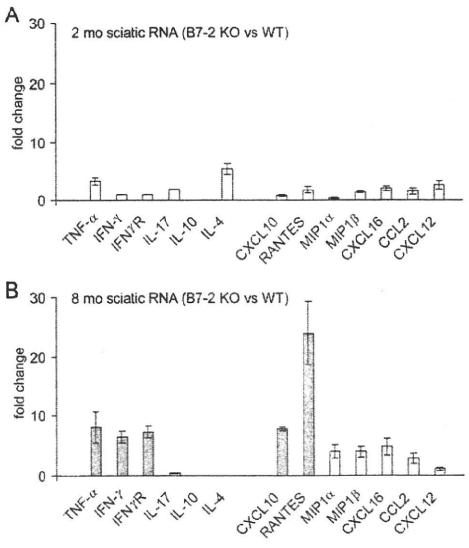


**FIGURE 2.** Comparison of cytokine and chemokine transcripts in sciatic nerves of B7-2 KO NOD mice vs WT NOD mice at 2 mo (*A*) and 8 mo (*B*). Data shown represent an average from three independent experiments except for 2-mo data on IFN-γ, IFN-γ receptor, and IL-17 ($n = 2$ each). There was a significant increase in the expression of TNF-α, IFN-γ, IFN-γ receptor, CXCL10, and RANTES in sciatic nerves of B7-2 KO NOD mice at 8 mo, when compared with age-matched WT NOD mice or 2-mo-old B7-2 KO NOD mice. Other chemokines were increased to a lesser extent. There was no increase in IL-17 transcripts in sciatic nerves at 8 mo. IL-10 and IL-4 transcripts were not detected.

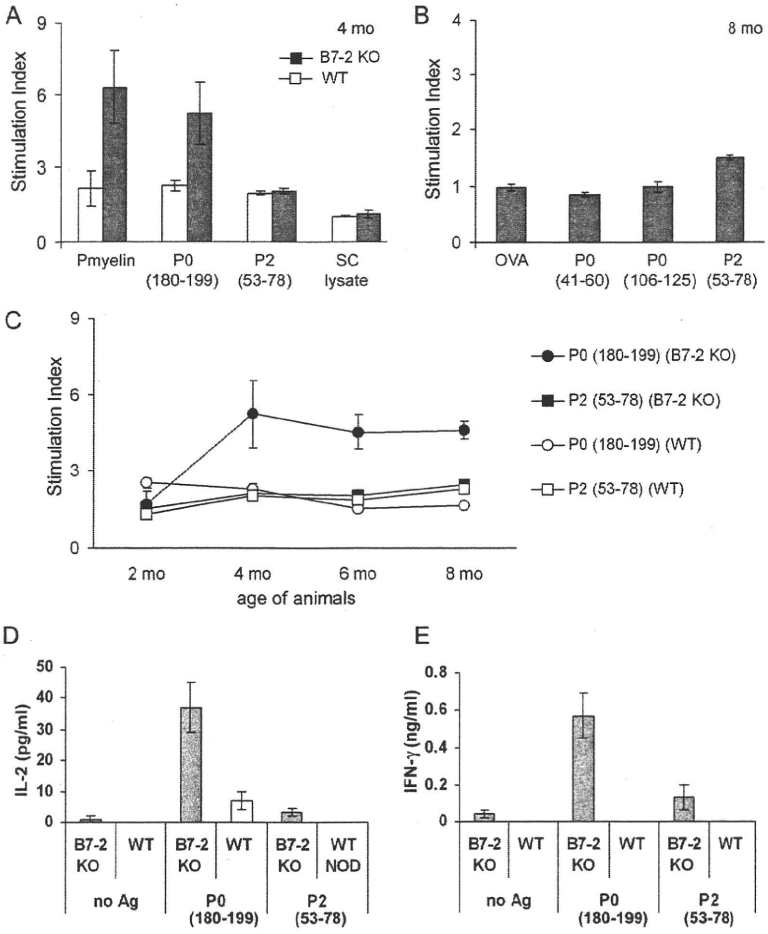


**FIGURE 3.** Splenocyte proliferative and cytokine responses to candidate SAP Ags. *A* and *B*, Splenocyte proliferation induced by PNS myelin (100 μg/ml), various P0 peptides (20 μg/ml), P2 (53–78) (20 μg/ml), SC lysate (100 μg/ml), and OVA (20 μg/ml). WT NOD (□) and B7-2 KO NOD (■) mice ($n$ = 3–4 each in *A*, $n$ = 3–5 in *B*) are shown. Results are expressed as stimulation index, with values >2.2 considered positive. Untreated at 1110–2468 cpm. *C*, Time course of splenocyte proliferative response to P0 (180–199) and P2 (53–78) in mice ($n$ = 3–4). *D*, P0 (180–199) but not P2 (53–78) stimulates the secretion of IL-2 and IFN-γ by splenocytes from B7-2 KO mice ($n$ = 3–4). Treatment duration was 72 h for proliferative response and 48 h for cytokine assays.

freeze (−80°C) and thaw (37°C) without detergents. Cultured neonatal rat Schwann cells were established as previously described (25).

### *Preparation of T cell lines and adoptive transfer studies*

Lymphocytes were isolated from spleens, axillary and inguinal lymph nodes of B7-2 KO and wild-type (WT) NOD mice using the Lympholyte-M gradient (Cedarlane Laboratoruies). Purified $CD4^+$ T cells were obtained using Dynal Mouse CD4 negative isolation kit (Invitrogen). To generate P0-specific T cell lines, $CD4^+$ T cells ($1.5 \times 10^6$/well) were cultured with $3 \times 10^6$ irradiated (3000 rad) syngeneic splenic APCs in the presence of P0 (180–199) (20 μg/ml) plus rIL-2 (25 U/ml) for 5 days followed by a 5-day resting period without Ag but with rIL-2 (25 U/ml). After three cycles of stimulation and rest, the specificity of the cell line was examined by proliferation assay in response to P0 (180–199) and control peptides. For adoptive transfer studies, P0-specific T cell lines were activated in vitro with P0 (180–199) for 3 days before injection of $6.5 \times 10^6$ cells into the tail vein of NOD.SCID mice. OVA-reactive T cell lines were generated from pooled splenocytes and lymph node cells of mice immunized with OVA (100 μg) in CFA by s.c. injections over four sites.

### *Real-time PCR*

The total RNA was isolated using a TRIzol reagent (Invitrogen), followed by Qiagen column purification. Reverse transcription was performed from 1 μg total RNA and the cDNA was used for SYBR green real-time PCR. Amplification was performed with forward and reverse primers for transcripts of interest, which was designed using Primer3 software. The expression of each cytokine or chemokine gene was normalized by corresponding amount of GAPDH mRNA for each condition. The relative amounts of each product were calculated by the comparative threshold cycle method ($C_T = 2^{-\Delta\Delta C_T}$) as described for the ABI Prism 7900 Sequence Detection System (user manual no. 2; Applied Biosystems). Primer sequences for real-time PCR studies are listed in Table I (supplementary data).[5]

### *Intracellular cytokine analysis*

Splenocytes ($10 \times 10^6$/well) in 6-well plates were stimulated at 37°C in a humidified $CO_2$ incubator for 4 h with Leukocyte Activation Cocktail containing PMA, ionomycin, brefeldin A, and BD Golgiplug. After culture, cells ($1 \times 10^6$) were stained for cell surface CD4 and intracellular IFN-γ and IL-17, using the Intracellular Cytokine Staining Starter kit (BD Pharmingen). The number of IFN-γ- and IL-17-producing $CD4^+$ T cells was analyzed by FACScan (BD Biosciences) and FlowJo software.

### *Western blot analysis and immunofluorescence studies*

Samples (equal amount per lane) were resolved by 12% SDS-PAGE and electroblotted to PVDF membranes. Blots were blocked with 5% nonfat milk in 10 mM Tris (pH 7.5), 100 mM NaCl, 0.1% Tween 20 for 1 h at room temperature. Blots were incubated with mouse Ab α P0 (1/3000; Astexx) or sera (1/200) overnight at 4°C, washed three times and then incubated for 1 h with goat anti-mouse IgG HRP-conjugated secondary Abs (1/5000; Calbiochem). In some experiments, isotype-specific HRP-conjugated secondary Abs (Santa Cruz Biotechnology) were used at 1/2000 to 1/10,000. Abs used for immunofluoresence studies include: mAb α P0 (1/500; Astexx); rabbit Ab α glial fibrillary acid protein (GFAP) (1/100–1/200; DakoCytomation); Alexa Fluor 488- and Alexa Fluor 598-conjugated secondary Abs (1/500; Molecular Probes).

### *Data analysis*

Results from real-time PCR experiments, immunologic studies, grip strength measurements and electrophysiology are expressed as mean ± SEM.

[5] The online version of this article contains supplemental material.

Statistical significance was determined by ANOVA followed by Student's $t$ test and the Bonferroni method for multiple group experiments. Significance levels were set at $p < 0.05$.

## Results

*Cytokine and chemokine profile in spleens and sciatic nerves*

B7-2 KO NOD mice begin to exhibit hindlimb weakness at 6–7 mo, progressing to generalized paralysis with time (3). To examine the cytokine and chemokine profile in spleens, real-time PCR studies were performed on splenic RNA from female B7-2 KO NOD mice at age 2, 4, 6, and 8 mo ($n = 3$ mice each). Results are expressed as fold change in gene expression compared with 2-mo data (calculated by the $2^{-\Delta\Delta C_T}$ method). As shown in Fig. 1*A*, there was a decrease in IL-10 transcript levels in spleens of female B7-2 KO NOD mice starting at 4 mo of age (preclinical phase). IL-17 transcripts peaked at 4 mo but declined toward baseline at 8 mo, whereas IFN-γ transcripts peaked at 8 mo (clinical phase) (At 4 mo, $p < 0.04$ for IL-17 vs IL-10; $p < 0.037$ for IL-17 vs IFN-γ, $p < 0.002$ for IL-10 vs IFN-γ. At 8 mo, $p < 0.003$ for IFN-γ vs IL-17 and $p < 0.01$ for IFN-γ vs IL-10). With regard to chemokines, there was a decrease in CCL2 transcript levels at 4 mo ($p < 0.004$ for CCL2 vs CCL3). There was no change in the levels of TNF-α, LT-β, IL-4, CCL3, CCL5 (RANTES), CXCL10 (IP-10), CXCL16 transcripts at any time points. For clarity, only four graphs are shown for each experiment (Fig. 1*A*). To determine whether changes in IFN-γ and IL-17 transcript levels correlate with functional polarization of Th cells, we examined the percentage of IFN-γ- and IL-17-producing $CD4^+$ T cells from the spleens of these mice by flow cytometry. Upon stimulation with PMA (10 ng/ml) and ionomycin (500 ng/ml) for 4 h, there was an increase in the percentage of $CD4^+$ IFN-$\gamma^+$ cells but not in $CD4^+$ IL-$17^+$ cells in splenocytes from B7-2 KO mice when compared with those from WT NOD mice at 6 and 8 mo (Fig. 1*B*).

For cytokine and chemokine profile in sciatic nerves, real-time PCR studies were performed focusing on two time points only (2 and 8 mo). Three independent experiments were conducted, and each sample consisted of pooled sciatic nerve RNA from three mice. TNF-α, IFN-γ, IFN-γR, CXCL10, and RANTES mRNAs were highly up-regulated in sciatic nerves of B7-2 KO mice at 8 mo compared with those from age-matched WT NOD mice, or to those from 2-mo-old B7-2 KO NOD mice (Fig. 2). A more modest increase in MIP1α, MIPβ, CXCL16, and CCL2 was also observed at 8 mo. There was no increase in IL-17 transcript levels in sciatic nerves of 8-mo-old B7-2 KO NOD mice when compared with WT NOD mice. These data suggest that Th1 cytokines, CXCL10 and RANTES are important mediators during the effector phase of SAP.

*Autoreactivity to PNS Ags in SAP*

We characterized the autoreactive T cell repertoire responsible for SAP by examining the proliferative response of B7-2 KO NOD splenocytes to PNS myelin (100 μg/ml), lysates of cultured neonatal Schwann cells (100 μg/ml), and two known neuritogens myelin P0 (180–199) (20 μg/ml) and P2 (57–81) (20 μg/ml). A stimulation index of >2.2 in the thymidine incorporation assay was considered positive. We observed a proliferative response to PNS myelin but not to lysates of neonatal Schwann cells (nonmyelinating), indicating that an autoantigen resides in peripheral nerve myelin or myelinating Schwann cells. Autoreactivity to P0 (180–199) was not detected at 2 mo, but was detected at 4, 6, and 8 mo (Fig. 3, *A–C*). Each data point represents the average from three to four independent experiments, each in triplicate wells. P2 (53–78), P0 (41–60), and P0 (106–125) did not induce a proliferative response ($n = 3$–5). Similarly, P0 (180–199) but not P2 (53–78) stimulates the secretion of IL-2 and IFN-γ by SAP splenocytes, as measured by ELISA ($n = 3$–4) (Fig. 3, *D* and *E*). There was no significant change in IL-10 or IL-17 secretion (data not shown). In contrast to B7-2 KO NOD mice, splenocytes from WT NOD mice exhibit minimal proliferative and cytokine responses to P0 (180–199) or P2 (53–78).

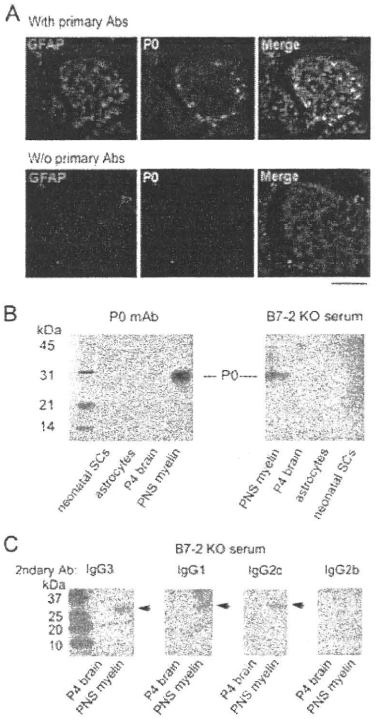


**FIGURE 4.** Expression of P0 by peri-islet Schwann cells and PNS, and autoantibodies to P0 in SAP sera. *A*, Immunofluorescence studies demonstrating that P0 expression was restricted to peri-islet Schwann cells, whereas GFAP was expressed by both peri-islet Schwann cells and Schwann cells infiltrating the islets. Scale bar represents 100 μm. *B*, Western blot analysis showing that the mAb α P0 used in *A* labeled a band at 28 kDa, the expected molecular mass of P0, in the lane loaded with PNS myelin. A similar band was labeled by B7-2 KO serum. Serum dilution was 1/200. *C*, Isotyping of anti-P0 Abs present in SAP sera. Serum Abs α P0 were of either Th1 or Th2 predominant IgG isotypes. Serum dilution was 1/200.

*Myelin P0-reactive T cells are involved in the pathogenesis of SAP*

Given that peri-islet Schwann cells, which express GFAP and S100β, are target of autoimmune attack in early insulitis (26), we examined whether these cells express P0 protein. Whereas the immunoreactivity against GFAP was observed in both peri-islet Schwann cells and Schwann cells infiltrating the islets of WT NOD mice, P0-reactive Schwann cells were restricted to the peri-islet region (Fig. 4*A*). Western blot analysis using a mAb α P0 identified a band at 28 kDa in the lane loaded with PNS myelin extract, but not in lanes loaded with lysates of cultured Schwann cells (nonmyelinating), cultured astrocytes, or postnatal day 4 brains (Fig. 4*B*). The same band was labeled by sera from B7-2 KO mice, albeit more frequently by sera obtained from 6- to 8-mo-old mice than those from 2- to 4-mo-old mice (8/8 (100%) vs 1/6 (16.7%)). Immunoreactivity was also detected occasionally by WT NOD sera (1/7 (14.3%)). Further studies revealed that serum Abs α P0 were of either Th1 or Th2-predominant IgG isotypes, with the frequency of IgG3 > IgG1 > IgG2c > IgG2b (Fig. 4*C*). It should be noted that IgG2a gene is deleted in NOD mice (27).